ISTANBUL TECHNICAL UNIVERSITY ★ GRADUATE SCHOOL OF SCIENCE ENGINEERING AND TECHNOLOGY

DESIGN AND OPTIMIZATION OF A RADON FIELD MONITOR BASED ON SILICON PIN PHOTODIODE

M.Sc. THESIS

Ahmet BAYRAK
(509091112)

Department of Physics Engineering

Physics Engineering Programme

Thesis Advisor: Prof. Dr. Cenap Ş. ÖZBEN

JUNE 2012

İSTANBUL TEKNİK ÜNİVERSİTESİ ★ FEN BİLİMLERİ ENSTİTÜSÜ

SİLİKON PIN FOTODİYOT BAZLI RADON SAHA MONİTÖRÜ DİZAYN VE OPTİMİZASYONU

YÜKSEK LİSANS TEZİ

Ahmet BAYRAK
(509091112)

Fizik Mühendisligi Anabilim Dalı

Fizik Mühendisligi Programı

Tez Danışmanı: Prof. Dr. Cenap Ş. ÖZBEN

HAZİRAN 2012

Ahmet BAYRAK, a M.Sc. student of ITU Graduate School of Science, Engineering and Technology student ID 509091112 successfully defended the thesis entitled **"DESIGN AND OPTIMIZATION OF A RADON FIELD MONITOR BASED ON SILICON PIN PHOTODIODE "**, which he prepared after fulfilling the requirements specified in the associated legislations, before the jury whose signatures are below.

Thesis Advisor :	**Prof. Dr. Cenap Ş. ÖZBEN** Istanbul Technical University	.....
Co-advisor :		
Jury Members :	**Prof. Dr. Serkant Ali ÇETIN** Doğuş University	.....
	Assoc. Prof. Dr. İskender A. REYHANCAN Istanbul Technical University	.....

Date of Submission : **4 May 2012**
Date of Defense : **8 June 2012**

" to my lonely and beautiful country which I love passionately ", N.B.C.

FOREWORD

First, I would like to thank to my family to support me in my academic career unconditionally. I would also like to thank to graduate student Esra BARLAS whom I work with in this project, Research Assistant Erhan EMİRHAN for his contributions. Finally, I thank to my advisor Prof. Dr. Cenap Ş. ÖZBEN for guiding me in each steps of this work, discussing the details and supporting me to materialize the radon field monitor. We appreciate TUBITAK for their support (110T261). The financial support by TUBITAK and İTÜ BAP division encouraged us to produce a radon monitor system, a product which we have already applied for a national PATENT.

8 June 2012

Ahmet BAYRAK
(Physics Engineer)

TABLE OF CONTENTS

Page

ABBREVIATIONS

MeV	**:** Mega Electron Volt
SCA	**:** Single Channel Analyzer
LLD	**:** Lower Level Discriminator
ULD	**:** Upper Level Discriminator
MCA	**:** Multi Channel Analyzer
ROI	**:** Region Of Interest
Ci	**:** Curie
Bq	**:** Becquerel
Gy	**:** Gray
Si	**:** Sievert
Rn	**:** Radon
U	**:** Uranium
Th	**:** Thorium
Pb	**:** Lead
PIN	**:** P-junction Intrinsic N-junction
HVPS	**:** High Voltage Power Source
DC	**:** Direct Current
pA	**:** Picoamper
V	**:** Volt
nA	**:** Nanoamper
PCB	**:** Printed Circuit Board
OP-AMP	**:** Operational Amplifier
JFET	**:** Junction Field Effect Transistor
mA	**:** Miliamper
HV	**:** High Voltage
kHz	**:** Kilo Hertz
IC	**:** Integrated Circuit
MΩ	**:** Mega Ohm
TTL	**:** Transistor Transistor Logic
MΩ	**:** Mega Ohm
Ra	**:** Radium atom
RMS	**:** Root Mean Square

LIST OF FIGURES

Page

DESIGN AND OPTIMIZATION OF A RADON FIELD MONITOR BASED ON SILICON PIN PHOTODIODE

SUMMARY

Radon is a member of natural radioactive decay series, U-238, U-235 and Th-232. Due to the formation of earth Uranium and Thorium are naturally present in the earth crust and therefore Radon.

Radon has several basic differences compared to most of the known radioactive atoms. It is in gas form, it does not have color and odour. Therefore when radon is produced under soil, it migrates to the earth surface through cracks by underground water sources. As a result of this, accumulation of radon in mines, tunnels and dwellings due to porous structure of building materials. Radon measurement can provide two results: First, long term continuous Radon measurement provide a relation between Radon level on the earth surface and seismic movements under soil. Second, we are exposed to Radon based alpha radiation during our daily life.

Unusual specifications of Radon make the detection process somehow difficult. Although there are several commercial devices for carrying out this task, due to their high prices investigations on this subject stay limited. In this work these devices are mentioned rarely. During this thesis we aimed to develop a low cost, electrostatic collection type Radon Field Monitor which includes all electronic parts, an alpha detector, a high voltage supply, a counter circuit and a data logging circuit, in a 30x30x40 cm metal cage. Besides, the device has the ability of operating with the energy supplied from both the mains power and a battery.

Alpha detector which uses a silicon PIN photodiode as the active surface, is the most important part of the Radon Field Monitor since it makes the detecion of Radon based alpha radiation. The alpha detector consist of three main sections: Transempedence amplifier, shaping amplifier stages and a comparator. Transempedence amplifier is a special way of amplifying very small signals as the output of the silicon PIN photodiode. However, the output of transempedence amplifier is not as big as to supply an information. Thus, by using a series of shaping amplifier stages the signal amplitude was increased. The obtained bigger signal is applied to a comparator IC and when it go beyond an adjusted threshold level it is converted to digital pulses. Then, it is possible to count the radiation signals. At the end all the elctronics of the detector located in a grounded metal cage to keep the very high amplification proceses against external electromagnetic noise.

The high voltage source which makes the biggest contribution to the measurement efficiency is the second important part of the device. The electronics of the high voltage source consists of an oscillator circuit, an amplifier circuit, a transformer, a Villard voltage multiplier, a load resistor and an RC filter group. A clock signal, generated in the oscillator circuit, is applied to the lower wounded input of the tarnsformer after a

pre-amplification process. Then, the amplified signal was both rectified and amplified in the Villard Voltage Multiplier stage. The load resistor and the RC filter circuit made the output stable. In the end the high voltage source supplied 3500V DC output. Besides by locating the circuit in a gorunded metal cage it was aimed to keep other circuits against the possible interference of clock signal.

Radon field monitor has four other electronic units supporting the operation. The sensor card is one of them making the atmopheric measurements by using a temperature sensor, a relative humidity sensor and an absolute pressure sensor. Device can operate by using the electricity from mains line and a battery located inside it against electricity break down. When the battery gets lower it can be recharged from the mains line or an integrated solar panel. All these operations are managed by another electronic unit. The counter unit is another electronic card in the device. Its only duty is to count the digital pulses coming from detector digital output. Then the counts are sent to a data loggin electronic unit and saved on an SD card in ".txt" format with date and time stamp. The datalogger unit is managed by a microprocessor which shows all operations on an LCD screen and let the measurement period to be determined manually.

Finally, after successfully testing the prototype device, 10 of the same unit have been produced and field measurements have been carried out in the basement of 4 Faculties in Ayazaga Campus of Istanbul Technical University.

SİLİKON PIN FOTODİYOT BAZLI RADON SAHA MONİTÖRÜ DİZAYN VE OPTİMİZASYONU

ÖZET

Radon, U-238, U-235 ve Th-232 doğal radyoaktif bozunma serilerinin bir üyesidir. Dünyanın oluşum sürecinden dolayı Uranyum ve Toryum elementleri ve aynı zamanda Radon yeryüzünün yapısında doğal olarak bulunmaktadırlar.

Radon, fiziksel özelliklerindan dolayı özel bir radyoaktif elementtir. Çünkü doğada gaz formunda bulunur ve rengi, kokusu ve tadı bulunmamatadır. Bu yüzden varlığının tespit edilmesi özel ölçüm cihazlarını zorunlu kılmaktadır.

Radon' un gaz formunda olması farklı getiriler sağlamıştır. Öyle ki yerin yapısında bulunan Uranyumun bozunumuyla oluştuğundan yeryüzünün derinliklerinde Radon oluşmaktadır. Oluşan Radon, yer kabuğundaki çatlaklardan ve yer altı su kaynakları yardımıyla yeryüzüne ulaşmakta ve yüzeyde bir konsantrasyon artışı meydana gelmektedir. Dolayısıyla bu durum iki sonuç doğurmaktadır: Birincisi, yer altındaki hareketlilikler Radon' un yer yüzüne çıkışını arttırıcı etkiler yapmaktadır. Radon seviyesinin sürekli takibi sismik hareketlilik hakkında bilgi sağlayabilir. İkincisi ise, yoğun Radon konsantrasyonu bulunan bir alanda, solunum yollarına yerleşen Radon ve Radon ürün çekirdekleri vücudun bu bölümlerinde kanser oluşma riskini arttırmaktadır.

Yirminci yüzyılın ikinci yarısından itibaren, Radon' un deprem habercisi olduğuna dair pek çok çalışma yapılmıştır. Bunlardan ilki Shiratoi tarafında 1927' de Japonya' da kaplıcalarda yapılmıştır [18]. Kaydedeğer bir sonuç ise ancak 1950' li yıllarda Hatuda tarafından yine Japonya' da elde edilmiş ve 8 şiddetinde bir deprem öncesinde ciddi Radon anomalileri gözlemlendiği bildirilmiştir. Bir başka önemli gözlem, Taşkent Özbekistan' da gerçekleştirilmiştir. Burada da yine yer altı su kaynaklarında yapılan ölçümlerde 5.3 şiddetinde bir depremden önce Radon anomalileri gözlendiği rapor edilmiştir. Yakın tarihli bir başgözlem bu defa Hindistan' da gerçekleştirilmiştir. 1999' da Chamoli' de meydana gelen 6.5 şiddetindeki deprem öncesinde 393 km uzakta bulunan ölçüm istasyonlarında kaydedilen Radon anomalileri Virk ve Walia tarfaından Rapor edilmiştir [27].

Radon' un sağlık üzerine etkileri, özellikle akciğer kanseri, uzun süredir araştırılan bir konudur. İlk çalışmalar, özellikle yüksek oranda Radon' a maruz kalan maden işçileri üzerinde olmuştur. Ancak 1980li yıllardan beri Radon' un toplumun geneli üzerine etkileri araştırılmaktadır. Bunların en önemli sonucu Radon' un sadece maden işçileri gibi yerin derinliklerinde çalışanlar için değil toplumun geneli için de akciğer kanseri sebebi olduğunun belirlenmesidir. Diğer bir önemli sonuç da Radon' un, toplumun genelinde, sigaradan sonra en büyük akciğer kanseri nedeni olduğunun belirlenmesidir. Bunun yanı sıra yüksek seviyede Radon bulunan ortamlarda yaşayan kişilerin sigara içmeleri, kanser riskini daha da arttırmakta olduğu da belirlenen başka biri durumdur.

Radon' un belirtilen fayda (deprem tahmini) ve zararları (akciğer kanseri), düzenli olarak ölçülmesini gelişmiş ülkelerde bir zorunluluk haline getirmiştir. Buna yönelik geliştirilen çeşitli Radon ölçüm yöntemleri ve bu yöntemlere göre çalışan çeşitli araç-gereçler dünya genelinde mevcuttur. Bu araç-gerçeler temelde aktif ve pasif olarak sınıflandırılabilecek iki tür yönteme göre işlevlerini yerine getirmektedirler. Aktif yöntemin en modern Radon ölçüm yöntemi olduğu söylenebilir. Bu yöntemle Radon ölçümü elektronik ve mekanik altyapıya sahip bir cihazşn kullanılmıyla gerçekleştirilir. Bu tür cihazlar genellikle ölçüm ortamındaki havanın örneklenip içindeki alfa ışımalarının sayılması prensibiyle çalışır. Ancak bazı firmalara ait, enerji ölçümü yapan cihazlar da bulunmaktadır. Bunun yanı sıra, dedektör kısmında yarı-iletken dedektörlerin yanı sıra iyonizasyon odacığı bulunan Geiger-Müller dedektörleri kullanan cihazlar da yine mevcuttur. Aktif Radon ölçüm yönteminin en önemli özelliği, ölçüm süresi boyunca ölçüm sonuçlarının sürekli takip edilebilmesidir. Böylece ölçümün başlangıç ve bitiş süreci arasındaki dönem hakkında da bilgi sahibi olunabilmektedir. Ancak olumsuz bir yönü, bu tür cihazların son derece yüksek fiyatlarla (bin dolarlar mertebesinde) satışa çıkmalarıdır. Diğer yandan, pasif yöntemde ise özel olarak hazırlanmaış bir kimyasal malzeme kullanılır. Herhangi bir elektrik beslemesine ihtiyaç yoktur. Ölçüm yapılacak alana yaklaşık 20 $ gibi fiyatlara satılan hazır bir aparat yerleştirilerek bir haftandan bir yıla kadar değişen sürelerde Radon' a maruz kalması beklenir. Farklı süreler kullanılan aparatın türüne göre değişmektedir. Belirlenen süre sonunda, aparat bulunduğu yerden alınarak, genellikle aparatı temin eden firmaya geri gönderilirek ölçüm sonucunun firma tarfından bildirilmesi beklenir. Bu süreçte firma aparatı bir takım kimyasal süreçlerden geçirerek analiz eder ve ölçümü sonuçlandırarak ilgiliye ölçüm sonuçlarını bildirir. Görece basit olan bu yöntemin de olumlu ve olumsuz yönleri bulunmaktadır. yöntemin olumsuz tarafı ölçüm süreci içinde Radon seviyesi hakkında bilgi edinilemez. Sadece tüm ölçüm dönemi hakkında genel bir sonuç elde edilir ve ölçüm sonuçlarına ulaşmak belli bir zaman almaktadır. Bunun yanında, son derece ucuz maliyeti ile gelişmiş ülkelerde, evlerde Radon seviyesinin belirlenmesi için, yaygın olarak kullanılan bir yöntemdir.

"Silikon PIN fotodiyot bazlı Radon saha monitörü" aktif yöntemle çalışan ve Türkiye' de sıfırdan üretilen ilk ve tarih itibariyle tek Radon ölçüm cihazıdır. Radon saha monitörü, aktif eleman olarak silikon PIN fotodiyotun kullanıldığı bir alfa dedektörü çevresinde şekillenmektedir. Detektör küresel simetrik güçlü bir elektrik alanın merkezinde bulunmaktadır. Bu amaçla bir yüksek gerilim kaynağı üretilmiş ve 3500V DC gerilim uygulanmıştır. Yarım küresel elektrik alan geometrisinin içine (ölçüm odası) bir hava motoru (1 lt/dk) ile gönderilen hava içeride oluşan basınç dolayısıyla dedektöre göre simetrik olarak bulunan başka bir açıklıktan ölçüm odasını terk etmektedir. Bu süreç içerisinde oluşan pozitif yüklü Radon ürün çekirdekleri fotodiyot yüzeyine taşınmakta ve burada alfa ışıması yapmaları sağlanmaktadır. Bu süreç içerisinde cihazda bulunan elektronik destek kartları ile cihaza besleme gerilimi sağlanmakta, ortamın atmosferik parametreleri ölçülmekte ve Radon sayımı ile birlikte tüm ölçümler bir SD karta kaydedilmektedir

Alfa detektörünün elektronik kısmı üç ana bölümden oluşmaktadır. Bunlardan ilki, fotodiyotta meydana gelen sinyalin yükseltildiği, yüksek kazançlı transempedans yükseltici, ikincisi sinyal şekillendiriciler ve son olarak da komparatördür. Fotodiyotun anot ve katodu arasında oluşan akım, uygun bir yükseltici olmadan gözlenemeyecek kadar küçüktür. Bu çok küçük akım ancak transempedans yükseltici ismi verilen özel bir yükseltici yardımıyla gerilime dönüştürülebilmektedir. Ancak yükseltilmiş

bu sinyal yine de ölçüm yapılabilecek düzeyde değildir. Bu yüzden bir şekil kuvvetlendirici dizisi kullanılarak sinyal genliği arttırılmaktadır. Elde edilen analog sinyalin genliği belli bir eşik değerini aştığında, şekil kuvvetlendiriciden gelen analog sinyal, bir komparatör yardımıyla dijital pulslara dönüştürülmekte ve radyasyonun sayılması mümkün olmaktadır. Detektör, çok yüksek kazançlı bir yükseltme işlemi yaptığından dolayı, elektriksel olarak topraklanmış bir metal kutu içerisine yerleştirilerek dış elektromanyetik gürültülerden yalıtılmıştır

Ölçüm verimine en önemli katkıyı sağlayan parçanın yüksek gerilim kaynağı olduğu söylenebilir. Yüksek gerilim kaynağı elektroniği bir osilatör devre, bir yükseltici devre, bir transformatör, bir Villard voltaj katlayıcı, bir yük direnci ve RC filtre grubundan oluşmaktadır. Osilatör devresinde üretilen saat sinyali bir ön yükseltmenin ardından transformatörün düşük sarımlı ucuna verilerek ikinci bir yükseltme gerçekleştirilmektedir. Ardından bu sinyal Villard voltaj katlayıcı devresinde doğrulma ve yükseltme işlemlerine birlikte tabi tutulurken en son çıkışa bağlanan bir yük direnci ve RC filtre grubu ile de çıkışın dengeli hale gelmesi sağlanmıştır. Sonuç olarak 3500V DC gerilim elde edilmiştir. Ayrıca devre topraklanmış bir metal kutuya yerleştirilerek, üretilen saat sinyalinin diğer devreleri etkilemesi engellenmiştir.

Radon saha monitörünün bu iki ana elemanı dışında, cihaza ihtiyaç duyduğu gücü sağlayan, atmosferik ölçümleri gerçekleştiren, dijital pulsları sayan ve tüm ölçümleri kaydeden elektronik kartlar da mevcuttur.

Güç seçici kart, iki farklı kaynak arasında cihazın besleme kaynağının otomatik olarak seçilmesini sağlayan elektronik birimdir. Öyle ki cihazın temel güç kaynağı 220V' luk şebeke hattı iken, elektrik kesintilerine karşın içerisine yerleştirilen bir akü ile de çalışmasına devam edebilmektedir. Bunun yanında akü sınırlı bir güç kaynaşı olduşundan terminalleri arasındaki gerilim belirli bir değerin altına düştüğünde şarj edilmesi gerekmektedir. Yine bu kartta bulunan bir şarj devresi ile akünün şarj olması da mümkün olmaktadır. Bu yüzden uzun süreli elektrik kesintilerinde ya da şehir merkezinden uzakta yapılan saha ölçümlerinde akünün şarj olması amacıyla cihaza bağlanabilen bir güneş paneli akünün şarj için gerekli olan güç kaynağı sorununu çözmüştür.

Atmosferik ölçümler, üzerinde birer adet sıcaklık, nem ve basınç sensörü bulunan bir sensör kartı ile gerçekleştirilmektedir. Sicaklik ölçümleri için National semiconductor firmasına ait LM35 sıcaklık sensörü kullanılmıştır. Ancak çünkü dinamik aralığı dolayısıyla bir OP-AMP yükseltici devre ile çıkış gerilimi yükseltilmiştir. Nem ölçümü için HSU-07C1-NMC3A isimli sensör kullanılmşıtır. Aktif elemanıyla birlikte küçük bir PCB kart olarak satılan bu sensör analog çıkış vermektedir ve çıkışına ayrıca bir işlem uygulanmamıştır. Basınç ölçümleri için de Motorola firmasına ait MPX200A kodlu mutlak basınç sensörü LMC660 OP-AMP ile hazırlanan bir sinyal düzenleme devresiyle birlikte kullanılmıştır.

Sayıcı devre, cihazda bulunan diğer bir elektronik birimdir. üzerinde 4 bitlik iki adet TTL sayıcı bulunan bir entegre devre elemanı sayım işlemini gerçekleştirmektedir. 8bit' lik dijital sayım sonucu bir dijital analog çevirici entegre devre elemanı yardımıyla 0-5V aralığında bir analog değere dönüştürülmekte ve veri kaydedici karta iletilmektedir. Veri kaydedici kart dört adet analog girişe sahip ve bir mikroişlemci ile kontrol edilen elektronik karttır. Dört girişine gelen her bir analog sinyali belirlenen periyotlarla, tarih ve saat bilgisi ile birlikte bir SD karta kaydetmektedir.

Ölçümler bir LCD ekranda eş zamanlı olarak görülebilmekte ve örnekleme süresi, tarih, dosya formatı gibi özellikler yine bu ekran yardımıyla ilgili tuşlara basılarak belirlenebilmektedir.

1. INTRODUCTION

The main source of the nuclear radiation is the unstable nuclide with excess energy in the structure of Earth itself, such as Uranium-238 and Thorium-232. After each radioactive decay, or nuclear disintegration, particles with varying energies, electrical charges and masses are emitted.

1.1 Radiation in General

In nuclear physics, there are mainly four types of radiations: Heavy charged particles, beta particles (electrons and positrons), X and gamma rays and neutrons. Each of them has different interaction properties with matter and each interaction results in different products.

Charged particles (protons, alpha particles or some other heavy ions) interact with any material in terms of their electric fields. This interaction results in an ionization or excitation of atoms in the material. After the ionization, ionized atoms and electrons travel some distance but electron travels significant amount of distance longer compared to the massive ions. The electrons can ionize other neutral atoms in their paths causing secondary ionization.

X and Gamma rays don't have electric charge. So the interaction between them and the sample material is much different than the case of charged particles. Therefore, the energy loss process of X and Gamma rays are examined under three main titles: Photoelectric Effect, Compton Scattering and Pair Production. Basically, Einsteins' famous formula explains the Photoelectric Effect and shows that when an incoming X or Gamma ray photon interacts with the electron of an atom in a target material, it transfers all of its energy to the atomic electron and take it apart from the atom. Generally, the free electron comes from K shell and when it leaves the atom, leaving a hole behind it. Then an electron in the L shell fills this hole and a characteristic X-ray is emitted. In the Compton Scattering, the energetic photon loose only some of its energy resulting the change of its trajectory. In the last process, photon interacts

with the electric field of a nucleus causing the creation of electron positron pair. The recombination of this pair results two gamma rays created back to back each having 511 keV energy.

In the Compton Scattering, the energetic photon loose only some part of its energy resulting the change of its trajectory. In the last process, photon interacts with the electric field of a nucleus causing the creation of electron positron pair. The recombination of this pair results two gamma rays created back to back each having 511 keV energy.

Interaction of neutrons are different than the other types of nuclear radiation. They interacts with matter through absorption, scattering etc...

1.2 Alpha Radiation

Researches about the alpha particle radiation has been done since the discovery of radioactivity by Becquerel. This is due to the radiation from naturally radioactive substances are mostly alpha emitters [1].

Alpha particle was discovered by Ernest Rutherford in the beginning of 20^{th} century during his researches on the Uranium decay [2]. He showed that an alpha particle is a Helium nucleus including 2 protons and 2 neutrons. Alpha particle was found to be the least penetrating radiation type because of its large mass (more than 7000 times that of a beta particle). Uranium, Radium and Radon can be given as example of alpha emitting radionuclides.

There are several reasons for occurrence of alpha decay. One of them is the large mass number of the natural radioactive series. In general, radionuclides with mass number greater than 150 are unstable and they decay alpha. In addition, ratio of the number of neutron to the protons is an important parameter to be considered [1].

The large binding energy of the alpha particle to the parent nucleus and its smaller mass than its constituents can be given as the second reason. The large binding energy let the atom release more energy by emitting an alpha particle and smaller mass makes the emitted particle to move faster, having larger kinetic energy [2]. In some decay types, the decay process needs some external energy. However in alpha decay, the parent nucleus release energy and the decay occurs spontaneously. Two decay processes of Thorium can be given as an example. Thorium (Th-228) - Radium(Ra-224) alpha

emission process, shown in Eq. (**1.2**), releases alpha with 5.5 MeV energy. On the other hand, Thorium (Th-228) - Actinium (Ac-227) proton emission process,shown in Eq. (**1.2**), needs to receive 6.4 MeV energy for the emission to be occurred [3].

$$^{228}_{90}Th \rightarrow {}^{224}_{88}Ra + \alpha \qquad (Q \simeq 5.5MeV) \tag{1.1}$$

$$^{228}_{88}Th \rightarrow {}^{227}_{87}Ac + p \qquad (Q \simeq -6.4MeV) \tag{1.2}$$

1.2.1 Mechanism of alpha decay

Alpha decay process has been explained by Gamow and independently by Gurney and Condon in 1928 [4]. They have given a quantum mechanical description for decay mechanism. Under the effects of both Coulomb interaction and nuclear force, an alpha particle is present in the nucleus confined in a potential barrier. The shape of the barrier is given in figure 1.1. The magnitude of the potential barrier decreases as getting away from the center of the nucleus.

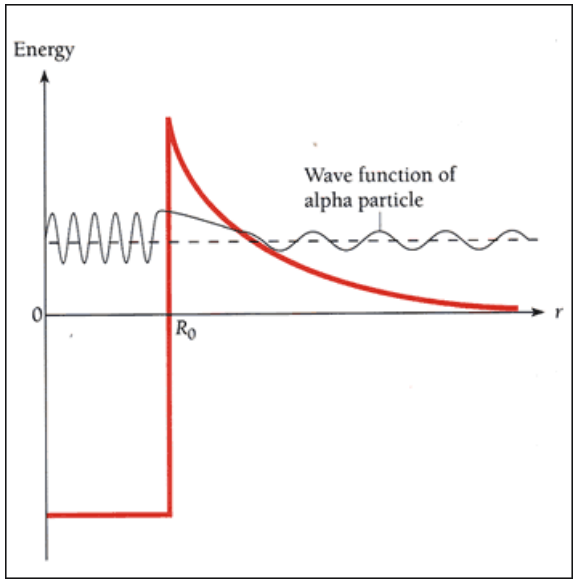

Figure 1.1: Alpha tunneling potential well.

Depending on the transition probability, calculated using the wave function, alpha particle have possibility to pass through the potential well, which named as tunneling. There is always a probability even it does not have enough kinetic energy. In the final stage, the mother nucleus loses 2 proton and 2 neutron which means a decrease of 4 in the mass number and decrease of 2 in the atomic number (Eq. **1.3**).

$$^{A}_{Z}X_N \rightarrow {}^{X-4}_{A-2}X'_{N-2} + \alpha \tag{1.3}$$

1.2.2 Alpha spectroscopy

Each alpha emitting radioactive nuclide has a characteristic alpha energies between 3-10 MeV. To be able to determine each radionuclide, spectroscopy is a powerful tool being used. The basic idea depends on the pulse height of the signals produced in the detector. The pulse height is determined by the energy of the incoming alpha particle.

Analyzer type being used and resolution of the spectrum are important issues in alpha spectroscopy [5]. A Single Channel Analyzer (SCA) is historically the earliest type of spectrum analyzer. It can observe alpha particles with a pre-determined energy. A single window is adjusted to the level of expected energy of alpha particle. This is provided by using a lower level discriminator (LLD) and an upper level discriminator (ULD). Because it is only possible to count the alpha particles at certain energy level, the analyst has to change the ULD and LLD levels manually to be able to scan the full energy span. However, today nuclear spectroscopy uses a much better tool, Multi Channel Analyser (MCA). An MCA consists series of individual SCA's. The analyst can observe the whole energy span at once and the spectrum quality is better when MCA is used. Spectra quality can be quantized with some parameters, like ROI and FWHM [5]. Number of channels in a MCA is directly related with the resolution of the spectra obtained. On the other hand, if analyst is interested in one specific energy interval, ROI (region of Interest) becomes useful. The term Full Width at Half Maximum (FWHM) is the signature of spectrum quality. The smaller the FWHM is better the resolution is [6].

Detector surface area is one of the most important parameters affecting the efficiency. Larger surface area let the device detect more alpha particles than the one with smaller area. It has to be remind that the alpha particles have very short range in air, the alpha spectroscopy has to be performed in vacuum. Vacuum level can be given as another important parameter related to the alpha detection efficiency. A good vacuum means less particles in the chamber. This leads less energy loss of alpha particles on average.

1.2.3 Energy loss of alpha particles in air and silicon

Accepting air is a gas, the energy loss can happen by excitation or ionization [6]. In an excited atom an electron changes its energy to higher level. However, an ionized atom loses one or more of its electrons and ion pairs are produced. On the other hand, this situation is different for semiconductors which has a band structure (Figure 1.2).

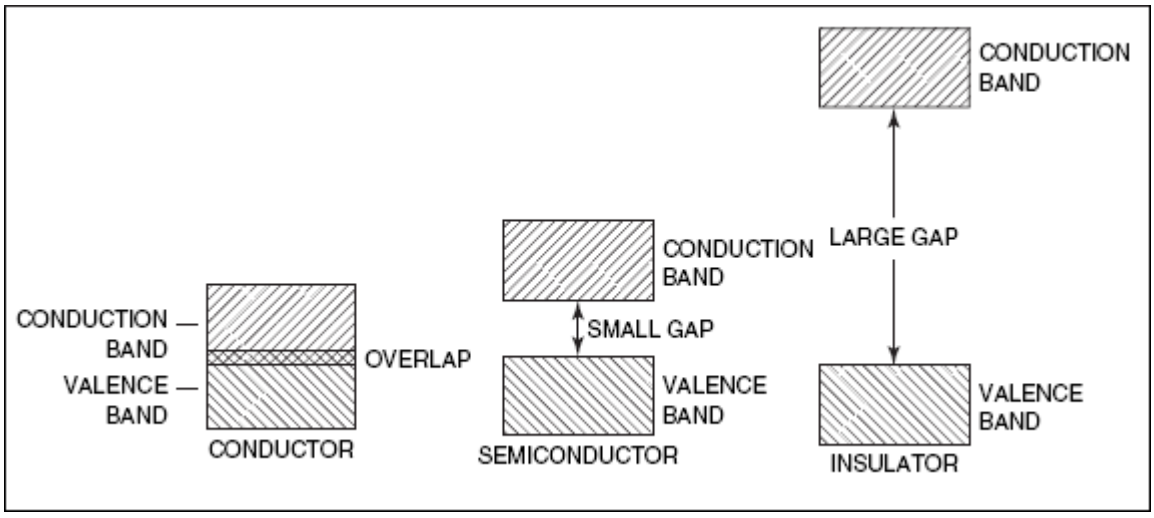

Figure 1.2: Semiconductor band structure [7].

In silicon, when an incoming charged particle pass through its lattice structure, electrons in the valence band of silicone migrates to the conduction band and electric current is produced. On the other hand, a charged particle produces electron hole pairs through its path which is similar to the ion pairs produced in the gas molecules [6].

Ionization becomes possible only when the energy of the incoming particle transfer a certain value of threshold energy to the valence electron of the material. During the passage of an alpha particle through a material, ionization can occur directly or indirectly by the interaction between liberated electrons and the material. This is called as secondary ionization.

The total number of ion pairs, produced per unit path length is called the Specific Ionization [8]. It is simply given in the following equation :

$$SI = \frac{\frac{dE}{dx}}{W} \tag{1.4}$$

where $\frac{dE}{dx}$ is the energy loss per unit length and W is the average energy needed to create a single ion pair [8]. The stopping power is the amount of energy which a charged particle loses along the length of its path. For alpha particle it is calculated as given in the following equation,

$$-\frac{dE}{dx} = \frac{4\pi Z^2 e^4}{m_e \upsilon^2} \tag{1.5}$$

$$= \frac{4\pi Z^2 e^4}{m_e v^2} NB \quad (\mathbf{1.6})$$

$$B = Zln(\frac{2m_e v^2}{I}) \quad (\mathbf{1.7})$$

where

υ: velocity of the charged particle

Z: charge of the charged particle

N: number density of the target

m_e: rest mass of the electron

I: experimentally evaluated average excitation and ionization potential

B: stopping number

2. RADON

Radon is a natural decay product of Uranium (^{238}U), Actinium (^{235}U) and Thorium (^{232}Th) decay series, existed since the formation of earth. Because of their very long half life, billions of years range, there is a great amount of Uranium and Thorium in nature today. This means there is Radon in the nature.

Each of these decay series results in an isotope of Radon, ^{222}Rn, ^{220}Rn and ^{219}Rn respectively. However, ^{222}Rn has a greater percentage to be able to detect due to its relatively long half life, 3.82 days [11]. Thoron, ^{220}Rn is also in detectable level in the nature.

In contrast with its parent nuclide, Radon presents in gas form in nature. Radon is a colorless, odourless and tasteless radioactive material [9]. These specifications make Radon difficult to detect and therefore dangerous for human life.

2.1 Radium Decay Line

As it is mentioned above there are three isotopes of Radon produced in three different decay chains. Most known Radon isotope is ^{222}Rn called as Radon. It is created in ^{238}U chain ending with stable ^{206}Pb atom. Since Radium is the parent nucleus, Radon formation is generally examined under Radium decay line shown in figure 2.1.

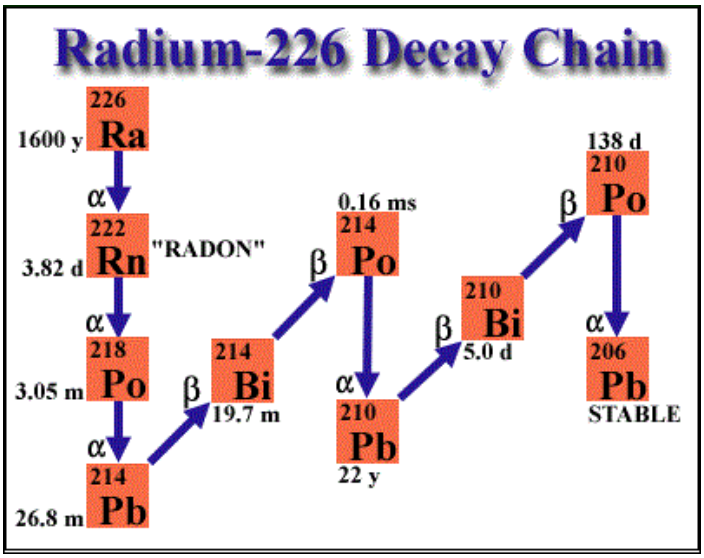

Figure 2.1: Radium decay line

2.2 Measurement Methods

There are certain methods for determination of radon concentration. Most of these are based on counting of alpha particles produced from the decay of Radon and Radon daughter products. These methods are examined under two basic tittles, passive methods and active methods.

2.2.1 Passive and active Methods

Passive Radon measurement does not indicate any device or need any user. Such detectors indicate a piece of material with the size of a human hand. Then if there is any Radon in that measurement area there happen some interaction between the alpha particles and the material depending on the type used. At the end of a given time period and after some chemical operations on the material, Radon concentration is determined [12].

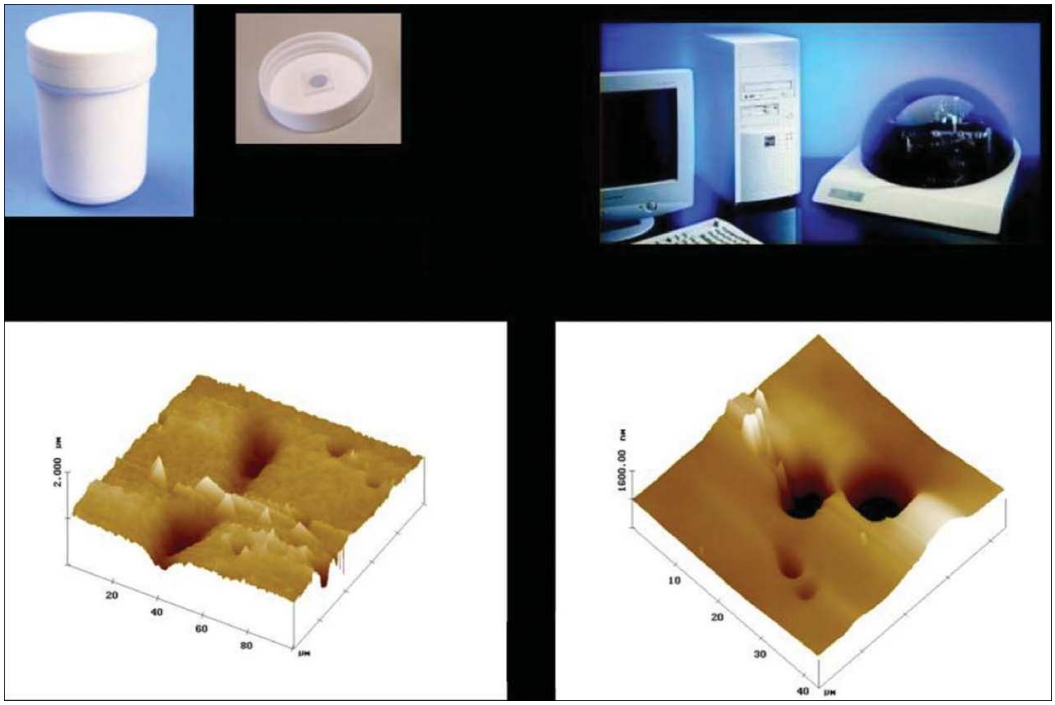

Figure 2.2: Top - Alpha track detector and the track counting microscope setup; Bottom - Tracks etched on the active surface results after measurement [13].

Alpha track detectors (Fig. 2.2) are the most known passive Radon measurement devices. They indicate a piece of plastic material as active area that is sensitive to alpha particles. It is inside a container and it should be located into the measurement area. When alpha particles interact with active region, they leave small tracks on the material. In the end of measurement period, around 3-12 months, and after some

chemical operations track concentrations are determined by microscope and the radon concentration is roughly determined [12].

Another known passive detector type is a piece of processed charcoal (Fig. 2.3). Similarly these are located to the measurement location. It is expected Radon will be adsorbed by the charcoal for about 2-7 days. Then the material is sent to a related laboratory, gamma ray spectroscopy with a scintillating detector is used to determine radon concentration [12].

Figure 2.3: Charcoal canister Radon detector

On the other hand, active Radon measurements are deeply different than passive methods. In this type of measurements, electronic devices are used. The devices are formed around an alpha detector, a counter circuit and a data recorder unit. Some of them can display the measurement online.

2.2.2 Advantages and disadvantages of Radon measurement methods

Both types of Radon measurements emerged from needs and thus both of them are still in use. Passive methods have advantage of easy to use and being cheap. In these days anybody can buy radon kits around 20$ from internet. Just by following the easy instructions on them anybody can locate it to a suitable location and start the measurement period. Generally the laboratory service is supplied by the seller and one can learn Radon level after the analysis provided by the seller. However, disadvantages of passive methods are poor precision of the measurement and delayed results. Active measurement has advantage of real time data monitoring. Therefore unlike the passive methods it is possible to observe the variations during measurement period. However,

to operate such a device an experienced user is needed. Although there are attempts to develop low cost Radon monitoring devices, price of such devices at the moment is much more than passive detectors, in the thousands of dollars range.

2.3 Environmental Effects

Although Radon is not the only radioactive source we are exposed during our daily life, it has the largest percentage in the distribution of natural background radiation over cosmic radiation (Fig. 2.4) [14].

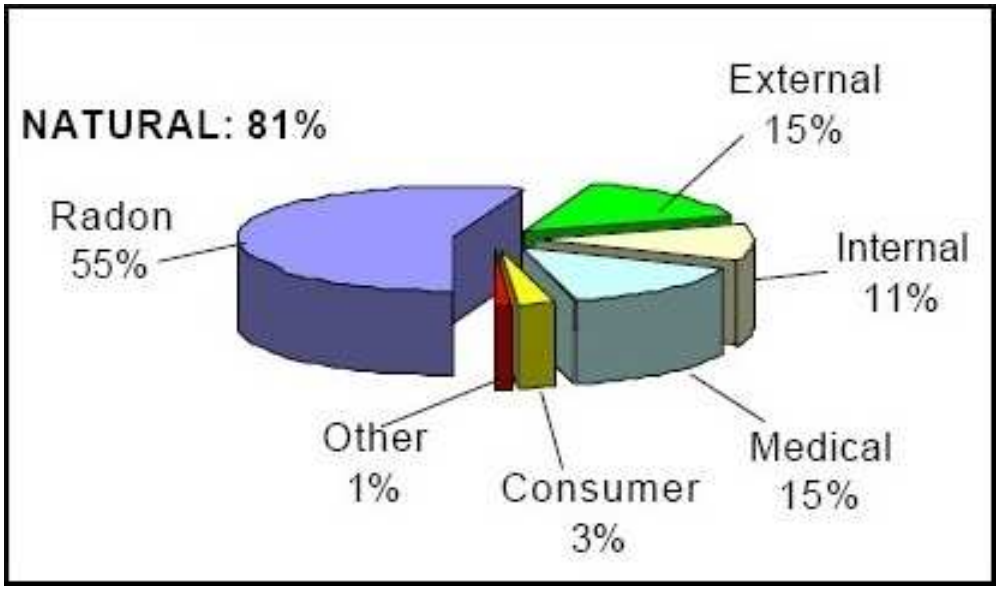

Figure 2.4: Ratio of background radiation [14]

2.3.1 Radon in living places

The gas nature of radon let it easily diffuse through different materials. This especially occurs in the Earth crust, the origin of Radon formation, due to the existence of Uranium and Thorium sources. The released Radon gas has several paths to reach to the Earth surface. Cracks in the Earth crust are one of the possible pathways and dissolution in the underground water resources is another one.

Radon that reaches to the Earth surface accumulates in especially underground locations due to the greater density than air (about 8 times). Cages, mines, subway tunnels and stations are several examples for such areas. However, buildings are the most important places about health effects of radon in where we spent much of our lives. Porous structure of building materials are also one of the reason of human exposure to Radon. Figure 2.5 shows the entry points of Radon to our homes. Possible cracks in the concrete and windows close to the soil level are possible migration ways

of Radon. Although basements can be the first place under risk, Radon can reach to the upper floors from the water pipes.

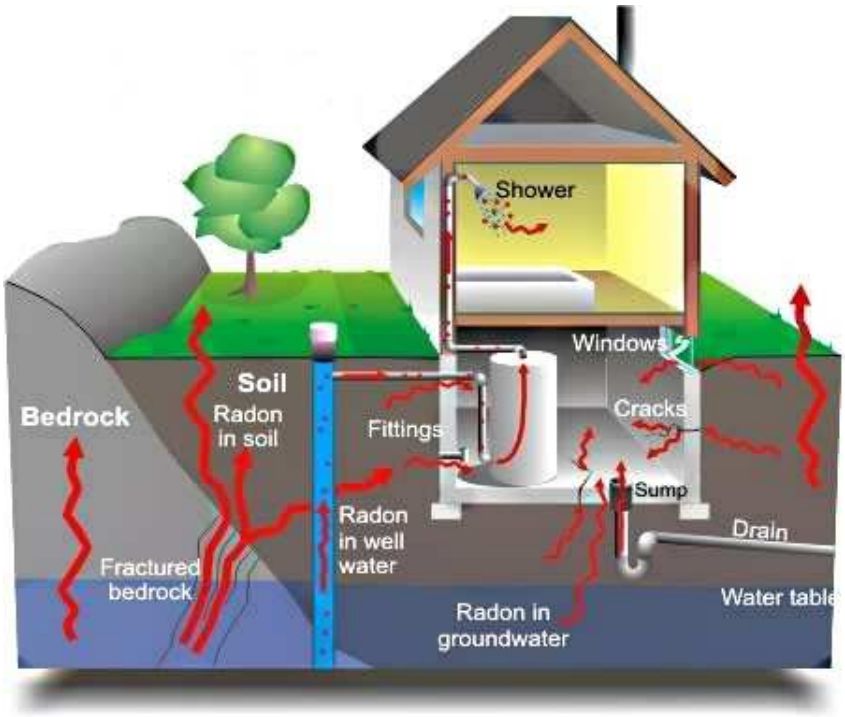

Figure 2.5: Pathways of Radon entering to the buildings [15].

2.3.2 Relation between Radon and lung cancer

Health effects of Radon have been investigated for about thirty years. First surveys have been done on the mine workers and in the early 1980's and some evidences have been found about the relation between radon concentrations and the lung cancers in the general population [16].

Although Radon is an alpha emitting radioactive substance, its ionic decay products, ^{218}Po and ^{214}Po, are also emitting alpha particles. Therefore, while Radon is inhaled, ^{218}Po and ^{214}Po deposit on the surfaces of the respiratory system which results in DNA damage. On the other hand, combination of smoking and Radon increases lung cancer risk [16].

2.4 Correlation Between Earthquakes and Radon Level

Since the second half of the 20^{th} century there have been quite a few works all over the world on the precursor signals of the earthquakes related to Radon [17]. However, later on some other ideas also appeared claiming that Radon measurement is a useful way of discovering the Uranium mines. Another claim is about the underground caves for the storage of natural gas, possibly bought from other countries. By discovering

the pathways it is possible to find the suitable areas for keeping the natural gas [13]. An interesting result of this, then it will be possible to store CO_2 which accepted as one of the reasons of global warming [13].

Initial investigations appeared in Japan since there happened so many strong earthquakes they give much care to this issue. In 1927, after his studies on hot springs Shiratoi came up with the idea, the relationship between Radon and the seismic activities [18]. After several decades, a remarkable observation obtained in 1953 by Hatuda on the measurements of Radon in the soil gas. At the end of a two years investigation on an active fault zone he reported a significant change on the Radon level, before the Tonankai earthquake with a magnitude (M) of 8.0 [19].

Later on in 1966, in a Tashkent artesian basin before an earthquake of M=5.3, a Radon anomaly was observed in a hot mineral water from aquifer, more than 1500m deep (Figure 2.6) [20].

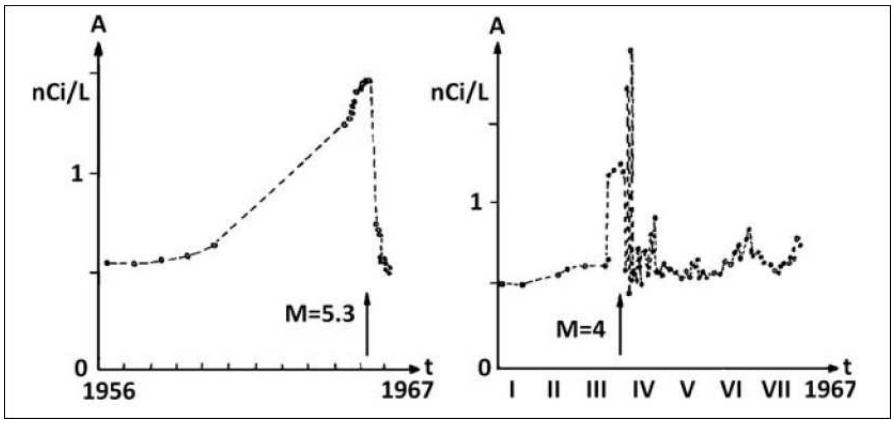

Figure 2.6: The Radon concentration variation in Tashkent and the correlation between two quakes (main quake and an after shock) and the Radon concentration [20].

Another study was carried out by Assimov and his group in somehow wide region. One of them was in Tashkent and the others were in Dushanbe, Alma-Ata, Andizhan area [21]. At the end, they found some signals designating the Markansu (1974; M=7.3), Gazli (1976; M=7.3) and Alma-Ata (1978; M=7.1) earthquakes. Radon anomalies related to these disasters was measured at a distance of 530 km, 470 km and and 65 km from the epicenter and 100, 4 and 50 days ago, respectively. Wakita and his group made a study at a 350 m deep well which is 25 km distant from the epicentre of Izu-Oshimakinkai earthquake occurred in 1978, M=7. In their paper, they reported that there have been an anomaly only 5 days before the quake [22].

Another considerable observation took place in Alaska between the years 1981-1983. Fleischer and Mogro-Compero carried out a measurement for two years at Near Sand Point [23]. They reported a correlation between a quake of M=6.3 and the Radon level variations measured about 180 km away of the quake epicentre. Again in 1983, Friedmann and his group made a study in soil gas on North Anatolian Fault Zone in Turkey and they reported varying Radon level before Biga earthquake M=5.7 [24].

In 1988, Hirotaka and his group cited an anomaly before Nagaro earthquake [25]. Three months ago, they cited a systematic increase of Radon concentration, however; there happen a serious increase before two weeks. And on 14 September, 1984 there happen an earthquake of magnitude (M) 6.8, 65 km away of the measurement site. In 1995, Igarashi and his group cited an anomaly almost one year before the Kobe earthquake [26]. At first they observed an increasing level of Radon. Then, they measured a bigger increase before 2 weeks which is followed by a fast decrease. And on 15 January, 1995 the Kobe earthquake (M=7.2) occurred.

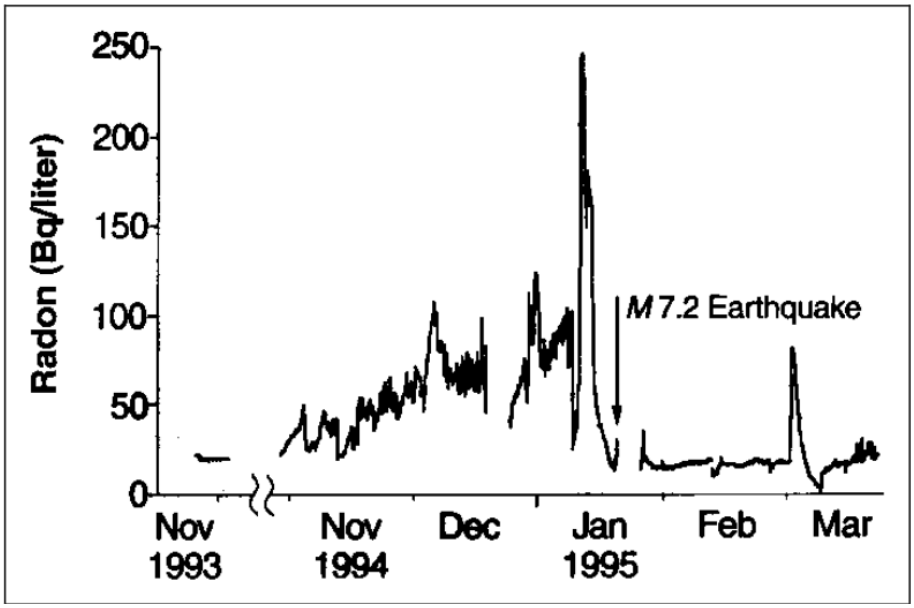

Figure 2.7: Radon anomaly before Kobe earthquake (M=7.2) [26].

In India, a different Radon anomaly was observed at Palampur measurement station about 393 km away of the epicentre of Chamoli earthquake, M=6.5, in 1999 [27]. The anomaly was observed before 19 days. Then 9 days before the quake Radon level reached to its minimum value and there have been a significant peak only two days ago.

Although, there are so many other examples since the foundation of the correlation between Radon anomalies and the seismic movements, investigators on this field could

not build a systematic relation. The most important topics which needs more and precise research are the relation between the measurement site and the epicentre of the quake, between the anomaly occurrence and the date of earthquake and between the atmospheric parameters and the measured data. All these investigations meet on just one point, an easy real-time measurement on as much as possible sites which needs a low cost Radon measurement device.

3. RADON FIELD MONITOR

The Radon Field Monitor is an active type radon measurement device consisting of several electronic cards, The silicon PIN photodiode alpha particle detector, The high voltage power supply (HVPS) and five other supporting electronic circuits, located inside a metal box. Each of five electronic circuit cards has different tasks, such as the management and regulation of the power sources, the measurement of atmospheric parameters (temperature, humidity and pressure) and etc...

The monitor has two gates to be able to get into. One of them is the cover screwed to the top of the box and the other one is a lockable door on the front side of the box (Fig. 3.1).

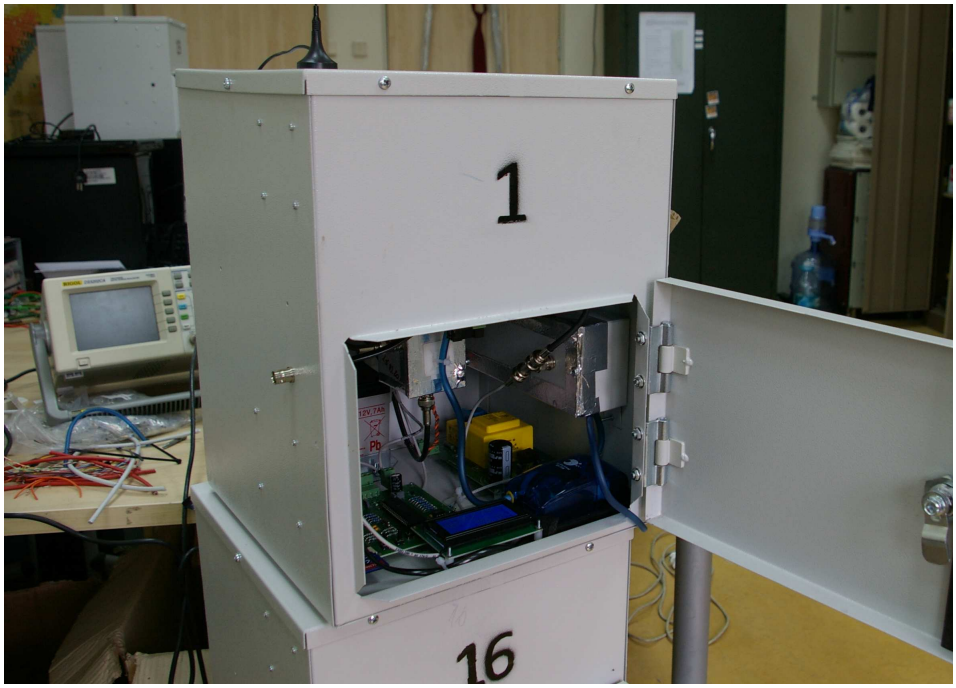

Figure 3.1: A general view of our Radon Field Monitor.

3.1 Parts of the Radon Monitor

The monitor has been separated into two parts, top and bottom, by using a wood shelf with 1 cm thickness. The top part is the place where the measurement is performed and the bottom part includes all the electronic cards and the Silicon PIN Photodiode Alpha Particle Detector. Because it has been fixed to the middle of the shelf between

two parts. Since +3500V DC high voltage is used, there is a need of isolation between the two parts to protect the electronics from the high voltage of collection chamber. Due to the financial requirements, 1 cm thick wood is used instead of plastics (Fig. 3.2).

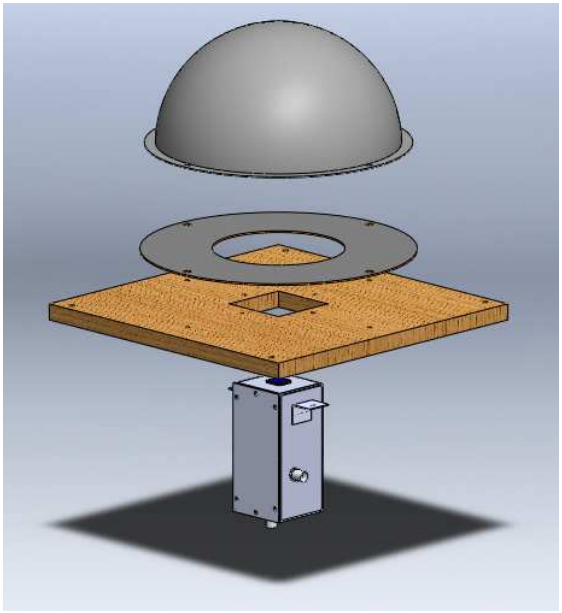

Figure 3.2: A solid design of the electrostatic collector.

In the top part and on the shelf, a metal hemispherical shell and a metal sheet with the same radius are concentrically located in the middle of the shelf. The metal sheet has 6 cm circular opening to locate the detector. There is approximately 2 cm distance between the detector and the metal sheet. There are two holes on the shelf for the connection of circulation lines for fresh air.

A sensor card, measuring the atmospheric conditions of the location, has also been there in this part, mounted to the inner side wall of the metal box.

In the bottom part, electronic circuit cards, those will perform the tasks needed during the measurement process, and the DC high voltage source are located. Those cards mentioned are power selector and distributor, the sensor, the logic counter circuit and the datalogger. The DC high voltage unit is a single module as the silicon PIN photodiode alpha particle detector, was mounted to the inner wall of the metal box.

3.1.1 Photodiodes

A photodiode is a semiconductor material which has a band structure. It means there are two different energy bands defining the material as insulator, conductor and semiconductor. While in insulators there is a large energy gap between valence and

conduction bands, there is almost no difference in conductors. Thus, in conductors electrons are free of moving in the conduction band due to the application of an electric field. However, in semiconductors, a relatively small energy is required to excite the electrons in the valence band to liberate them.

This energy comes from somewhere outside, from a photon or in our context from an alpha particle. Although photodiodes are actually photon detectors which creates relatively small signal depending on the energy of the incoming photon, it is also possible to detect charged particles.

3.1.1.1 P-N photodiodes

As it was described in the previous chapters (photoelectric effect), when a photon strike a surface it must have more than a threshold energy to be able to break the bond between the valence electron and the material atom. In this case, energy difference corresponds to the band gap between valence and conduction bands. In silicon, a common semiconductor materiel, 1.17 eV of energy is required to liberate an electron. In germanium, another popular material for semiconductor devices, (Ge) it is 0.775 eV. On the other hand, in diamond, a good insulator, there is band gap of 6 eV. If we apply an external voltage, bias voltage, then it is possible to make the electrons flow through the desired path.

Photodiodes are actually photon detectors which creates relatively small signal depending on the energy of the incoming photon. However, it is also possible to detect charged particles.

To be able to understand the principle of operation of a photodiode, understanding the P-N junction is a good point to start. Then it is possible to understand how the P-I-N photodiodes, are operating. Although each of them work in a similar manner, depending on the internal structures they differ in efficiencies.

Polarization of a P-N junction is the most important part of diode operation. In a common diode, positive voltage is applied to the P type material and negative to the N type. Then this let the current flow through anode to the cathode not to the reverse. However, in photodiodes the flowing electrons is just produced in the P-N junction itself. This is achieved by applying the positive and negative voltage in the reverse manner, called reverse biasing. In this way a region, called depletion region, between

P and N type materials is composed. When an incoming photon strike to the bonded electrons in the depletion region, it produce electron-hole pairs. Then a flow of charge carriers, current, is constituted. Even it is possible to create charge carriers without bias voltage, reverse biasing enhances the amount of generated electron-hole pairs.

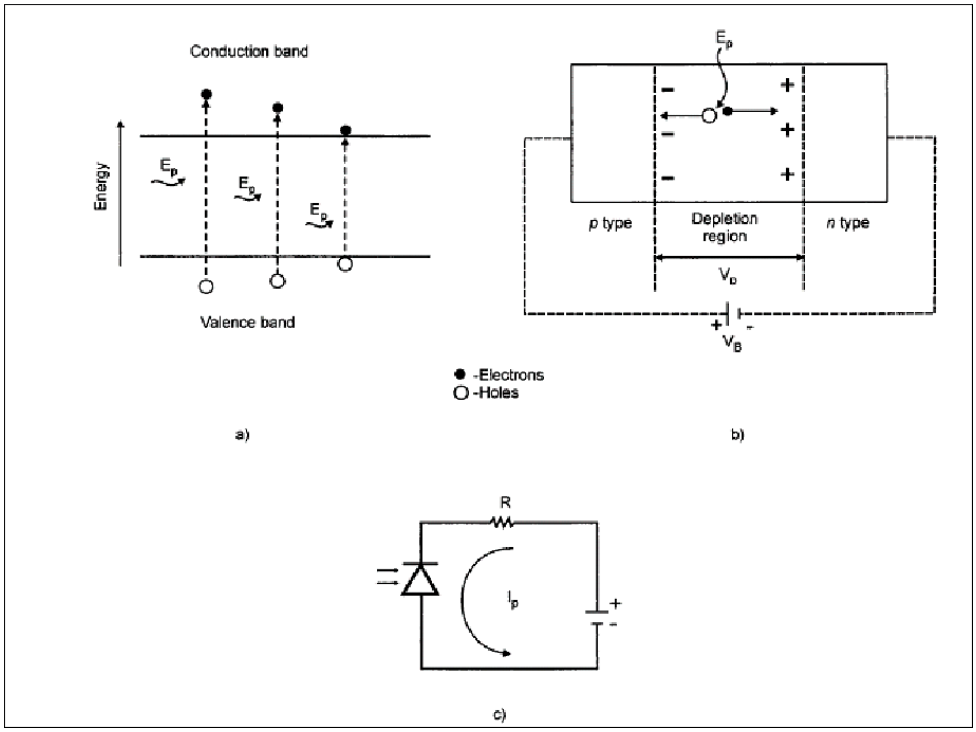

Figure 3.3: The principle of operation of a photodiode a) Energy-band diagram b) P-N junction (c) Electrical circuit.

3.1.1.2 Power relationship

The assessment of a photodiode can be made according to its response to the incoming radiation power and photon frequency. While the light power describes the input/output relationship, the frequency of the incoming photons provides the operating bandwidth of the photodiode.

When we consider power characteristics of a photodiode we need quantitative values. In this context, we consider *light power* (P) and *photocurrent* (I_P) as our quantities. Power is another definition of the number of photons as our input, and the photocurrent as our output. It is possible to deduce that the more the incoming photons strike to the active region, bigger the photocurrent will be produced as stated in Eq. **3.1**.

$$I_P = R.P \tag{3.1}$$

The slope of the equation provide an important and basic information about photodiodes, the *responsivity*, R (A/W) (Figure 3.4-a).

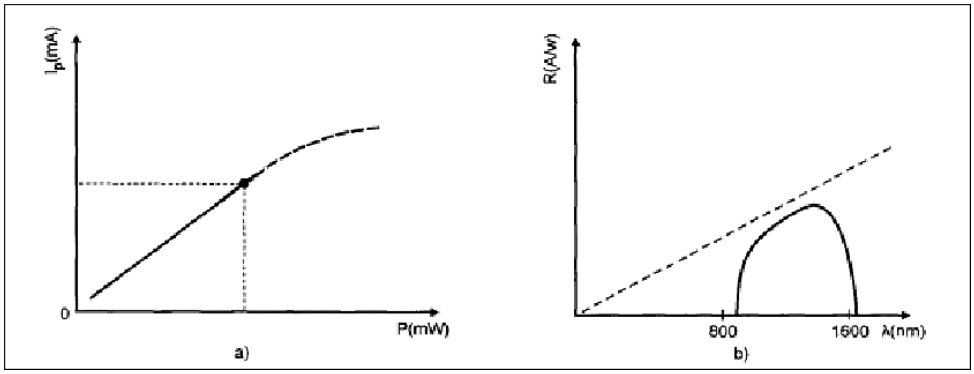

Figure 3.4: Photodiode responsivity a) input-output characteristics b) Responsivity due to wavelength.

Because responsivity let the user find out how efficient a photodiode in a given light power. Responsivity values are given by the manufacturers in the device datasheet. Generally they are very linear in some determined region; however, they also have a saturation level in where it is not possible to use the Eq. **3.1**. Power limits are determined at the production stage.

Responsivity is not only determined by the light power, but also the wavelength of the incoming particles which is an important case (Figure 3.4-b). As we noted above that the responsivity is the ratio of photocurrent to the light power. The basic definition of power is the energy per unit of time. Then we can write that;

$$P = \frac{N_P E_P}{t} \tag{3.2}$$

where N_P is the number of incoming photons and E_P is the individual energies of incoming photons. "t" denotes the time. Then we can also write the individual photon energies by Plancks' Law;

$$E_P = \frac{hc}{\lambda} \tag{3.3}$$

where "h" is the Plancks' constant $(= 4.136x10^{-15} eV.sec)$ and the "c" is the light speed $(= 3x10^{8} m/sec)$. In the last step we can write the photocurrent in a somehow basic form,

$$I_P = \frac{N_e}{t} \tag{3.4}$$

where N_e denotes the number of electrons liberated and "t" is again the time. Then combining all of these and rewriting the responsvity, we get;

$$\begin{aligned} R &= \frac{I_P}{P} && (3.5)\\ &= \frac{\frac{N_e}{t}}{\frac{N_P.E_P}{t}} && (3.6)\\ &= \frac{N_e}{N_P}.\frac{\lambda}{h.c} && (3.7) \end{aligned}$$

Something important appears here, the ratio of number of produced electrons to the number of incoming photons, named *Quantum efficiency* (η). It is an important parameter for detection systems. Because quantum efficiency shows how efficiently the active element is working. Then, *h.c = 1248 eV.nm*, is also a known quantity. When we combine all these again and rewrite the last equation of responsivity we get,

$$R = \frac{\eta}{1248eV.nm}.\lambda \tag{3.8}$$

For further description of the responsivity/wavelength relation, we can directly approach from the wave nature of the photons. When light reaches to the active surface of a photodiode, some of it will be reflected and some will be adsorbed. From the exponential attenuation relation, we can write that;

$$P_{abs} = P_{in}(1 - e^{\alpha_{abs}.w}) \tag{3.9}$$

where P_{abs}, P_{in} are absorbed and incident light power. "α" is the absorption coefficient and the "w" is the width or thickness of the active region, that's depletion region in our case. We can calculate the quantum efficiency from here, too. By dividing absorbed power to the incident one, we get

$$\begin{aligned} \eta &= \frac{P_{abs}}{P_{in}} && (3.10)\\ &= (1 - e^{\alpha_{abs}.w}) && (3.11) \end{aligned}$$

The most important result of the Eq. **3.11** is that it is possible to increase the quantum efficiency increasing depletion region width which can be controlled during the application.

On the other hand, the responsivity and the wavelength of the incoming photon has a linear dependence. However, there is something different on the Figure 3.4-b which shows the expected (dashed line) and real relation. In the graph there are two cut-off wavelengths at two edges. The reason for longer wavelength cut-off is the lack of enough energy to excite the valence electrons. The shorter wavelength cut-off is due to greater energy of the incoming photons. In this way photons will strike the electrons far from the energy gap edge and the probability of the exciting these electrons at the conduction band is very low.

A photodiode has the ability of working with or without bias voltage. Light carry enough energy to jump an electron from the valence band to the conduction band, thus it can generate current without bias voltage which is called *photovoltaic mode* (Figure 3.5 left). This is how the solar panels are working. In this mode dark current is minimum but it works with low speed. In *photovoltaic mode* (Figure 3.5 right) it is needed to apply an external bias voltage which we used also. Although the speed is high in this mode, the dark current is also high.

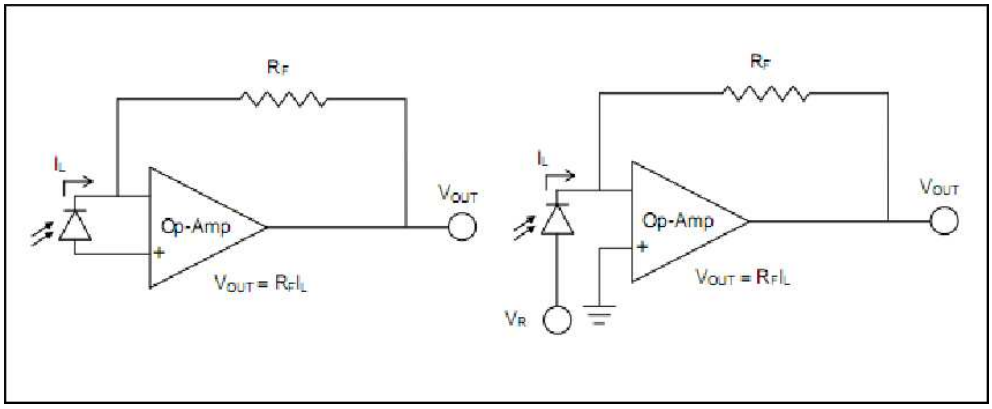

Figure 3.5: Photodiode theory of operation: photovoltaic mode (left) and photoconductive mode (right).

Application of a reverse bias voltage has several advantages. Generated internal electric field, the main support of the fast response, is one of them. When the incident photon generate free charge carriers in the depletion region, the applied voltage separate them and produce the photocurrent. If the electron-hole pairs created in p or n regions because the lack of electric field they will move slowly. However,

the reverse bias in the depletion region make the charge carriers move fast. Thus the photocurrent created in depletion region is called *drift current* and in *p* or *n* region is called *diffusion current*. Besides, in depletion region even there is no incident photon, some charge carriers can be created due to the thermal effects. In the electric field they produce some amount of current, called especially because the lack of any light, *dark current (I_d)*. It is an unwanted signal in any detection device determining the sensitivity of the device. Although, with the usage of reverse bias it is possible to control the dark current, we cannot choose the bias voltage value arbitrarily. Instead, we can use a P-I-N photodiode which has a steady depletion region inside called intrinsic region.

3.1.1.3 P-I-N photodiodes

PIN photodiodes differ only at the internal structure from the PN photodiodes. PIN photodiodes consist of a single crystal having an undoped intrinsic region sandwiched between p and n types. PIN photodiodes are also photon detectors where they are sensitive to the wavelengths between 250 nm and 2 μm depending on its base material. Since the intrinsic region naturally thick, generation of free charge carriers has a greater probability than PN photodiodes. Then this results in high quantum efficiency. Since there is no need to adjust a reverse voltage for widening the depletion region, they have also high power and bandwidth efficiency.

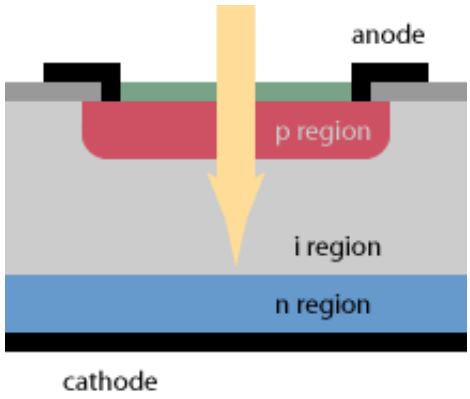

Figure 3.6: PIN photodiode internal structure.

In PIN photodiodes, generated electron/hole pairs are efficiently collected due to the strong electric field in the active region. This is achieved by the lack of free charge carriers. Besides, as it was mentioned before, the reverse bias decreases the dark current by pushing electrons originated from the thermal effects. Because the P and N regions are very thin, incident photons less likely enter these regions and the diffusion current becomes very small. This result in the increase on the bandwidth efficiency.

Specific ionization of alpha particles is relatively high and alpha particles induce relatively large current compared to gamma rays in silicon PIN photodiodes. Energy loss mechanism of the alphas is based on the electronic excitation and the ionization. Alphas from natural radionuclides have energies between 4 and 10 MeV and loose almost all of their energy in the base material (typically few hundred microns thick) of the PIN photodiode. This makes the detection efficiency nearly 100%.

Active area, maximum reverse bias voltage, thickness of the depletion layer and the dark current are some of the important considerations for the choice of a proper photodiode. Silicon Sensor PS100-7-CER-2 PIN photodiode (Fig. 3.7) comes with ceramic package has an active area of 100 mm^2, can handle reverse bias voltage up to 50 V and has 5 nA dark current at 12 V. Any other photodiode with the similar specifications and the price would also work for our purpose.

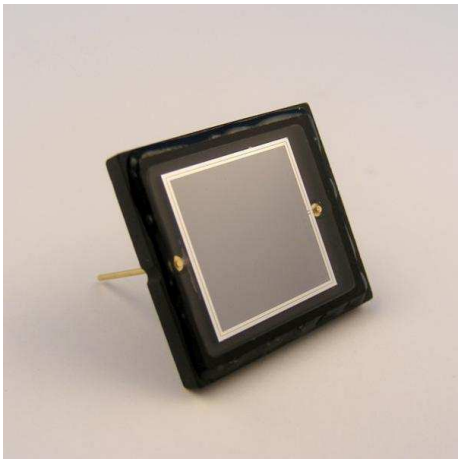

Figure 3.7: PS100-7-CER-2 PIN photodiode

3.1.2 The Silicon PIN Photodiode Alpha Detector

Detector is the most important part of the device and the detection circuit is based on a Silicon PIN Photodiode which produces a current signal against the radiation. Then this very small current is converted to a voltage via a shaping amplifier stage. The alpha detector provides digital output and also amplified output for MCA purposes.

3.1.2.1 The PIN Photodiode amplifier

The most important part of the detector is definitely this section since it is the heart of the detection system. Reducing the noise, obtaining the optimum shielding and finding the best design of the PCB were the main issues for this part of the radon monitor. Photodiode amplifier has three main sections. These are the transempedance

amplifier, the shaping amplifier and digital output. An amplified output for MCA also takes place for mainly the gain and the threshold adjustments of the amplifier and the comparator.

A transempedance amplifier (Fig. 3.8) in the detection circuit was used for converting the induced photo-current into the voltage. The current generated by alpha particles in silicon is many orders of magnitude larger compared to the one generated by gamma rays as it was pointed out. Therefore, noise due to dark current caused by internal resistance of the photodiode, the number one problem for the detection of X or γ rays, becomes almost irrelevant for the detection of alpha particles. This obviously makes the things easier for the radon monitor.

The internal capacitance of the photodiode slows down the detection. Application of DC reverse bias voltage over a large resistor R_b expands the depletion region and this increases the detection probability. Finally, to obtain a stable output signal, a feedback capacitor C_F was added to the circuit (Figure 3.8). This circuit is pretty much standard and it is called as transempedence amplifier.

To convert the induced current to voltage, an ultra low noise OP-AMP or a JFET must be used in the first stage of the amplification. It is not difficult to find OP-AMPs with excellent noise specifications today.

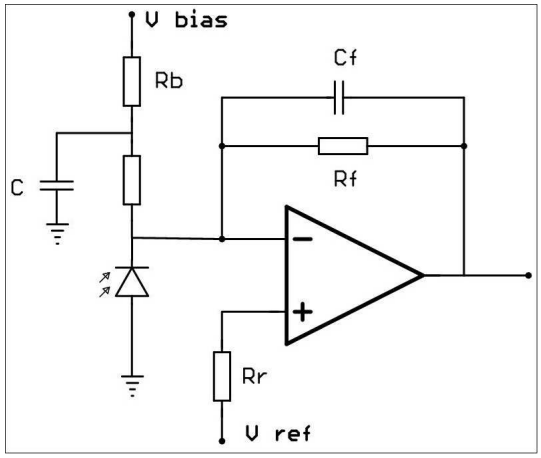

Figure 3.8: Transempedance amplifier

These OP-AMPs are the ones with JFET input stages. The input current noise density i_n, the input voltage noise density e_n, input capacitance C_{in} and input bias current I_B are the most important parameters for choosing the most suitable OP-AMP. Going through the various manufacturers, MAX4478 and LMC660 were chosen to be used for our final design.

Following the transempedence amplifier stage, three other identical stages take place for shaping the signal. Figure 3.9 shows the shaping amplifier stage. The choice of the feedback capacitors in every stage of the shaping amplifier were experimentally optimized for improving the signal shape and the count rate. This work was performed using a ^{226}Ra alpha source.

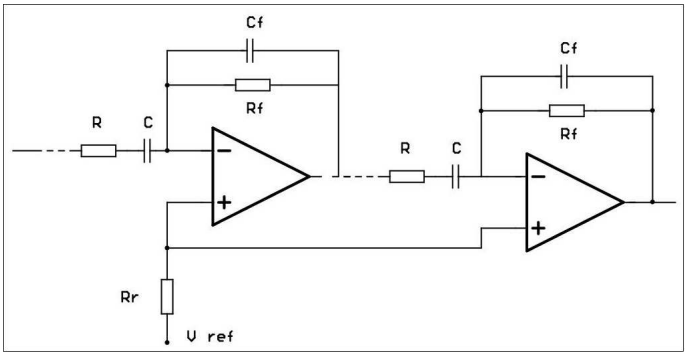

Figure 3.9: Shaping amplifier

Since amplification gain was large in the first stage, at least this stage was shielded properly. Because of the sensitivity of the photodiode to the light, the detection chamber was shielded against any light leakages.

The output of the shaping amplifier (typically few hundred milivolts) was not capable of driving an MCA. For that reason, another OP-AMP was used for amplifying the signal to Volts level. The complete photodiode amplifier circuit drains only 18 mA current in 5V DC.

3.1.3 High Voltage Power Supply

Due to very low range of alpha particles in air (usually couple of cm), only the alphas near the photodiode reach to the detector and generate signal. This situation greatly reduces the detection efficiency of the radon which is already low in concentration under regular circumstances. However, it has been known that when radon decays, the daughter nuclei, ^{218}Po (and later on ^{214}Po) are highly ionized. Most of these ionized atoms attach to the other ionized dust particles in the environment and they can be drifted to the photodiode with the help of a strong electric field. For that reason, a DC high voltage power supply was needed to provide the necessary electric field. The ripple from HV source was only 0.3% of 3500 Volts. Electric field generated from

3500 V was decided to be good enough to obtain a reasonable collection efficiency.

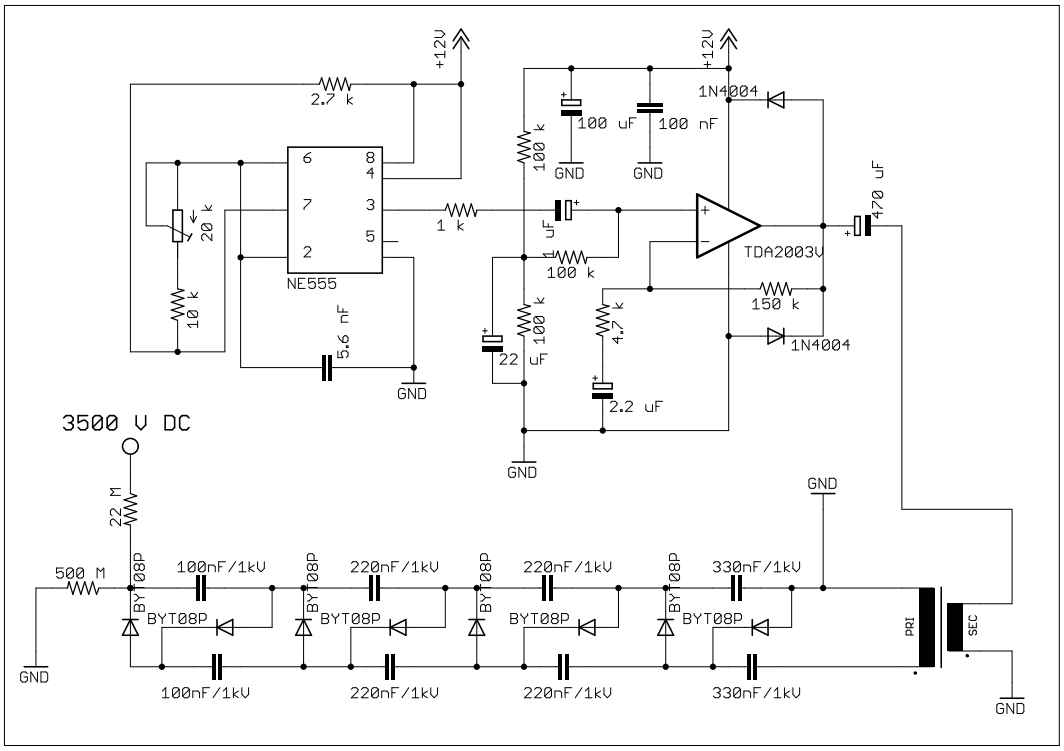

Figure 3.10: DC High voltage power supply circuitry

The high voltage circuitry (Fig. 3.10) is based on the Villard cascade voltage multiplier circuit. An NE555 oscillator with an adjusted 9 kHz square wave with 50% duty cycle was amplified with a TDA2030 audio frequency amplifier. This IC was designed to drive low empedence but highly inductive loads like speaker, somehow similar to the primary or secondary winding of a 220V/6V transformer. A stepped up 440 volt generated from the primary winding of the transformer was then cascaded to nearly 3500 V with a 4 stage multiplier. A 500 MΩ resistor was connected between the last stage of the multiplier and the ground for the stability and the output was filtered with a series RC filter.

3.1.4 Power Selector and Distributor Circuit

Device can operate by using to power sources: The mains power and a battery. Besides we have connected a solar panel against operation in the field where there is no mains power line. This section provides an automated transition between these two power sources (Fig. 3.11). When the mains power is available, the power needed by the radon monitor is supplied from the mains and the battery is charged. When the mains power is not available, the battery is connected to power the monitor and it is charged from the solar panel in the presence of the sun light. The importance of this unit is to make the device go on to operate without any break both in field and/or rural areas.

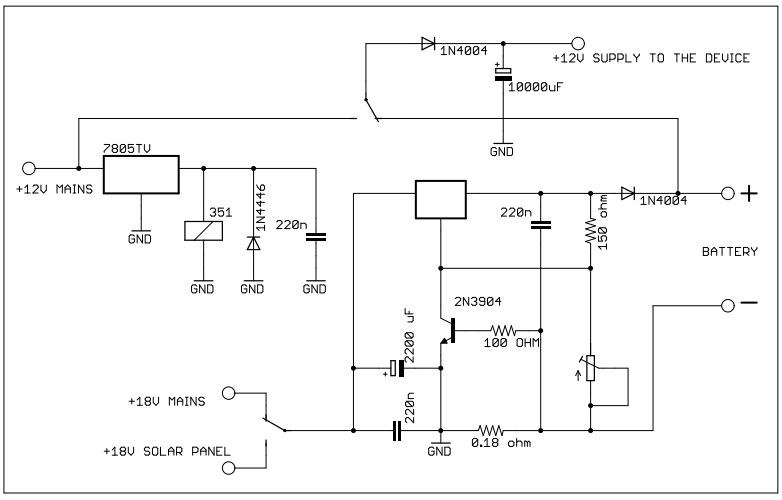

Figure 3.11: The power selector and distributor circuitry

3.1.5 The Sensor Circuit

Measurements of temperature, humidity and absolute atmospheric pressure of the environment are required due to the correlations between the level of these environmental parameters and the detected radon level. For this reason, these parameters should be measured continuously in addition to the measurement of radon level and the necessary corrections were applied to the data in the analysis stage.

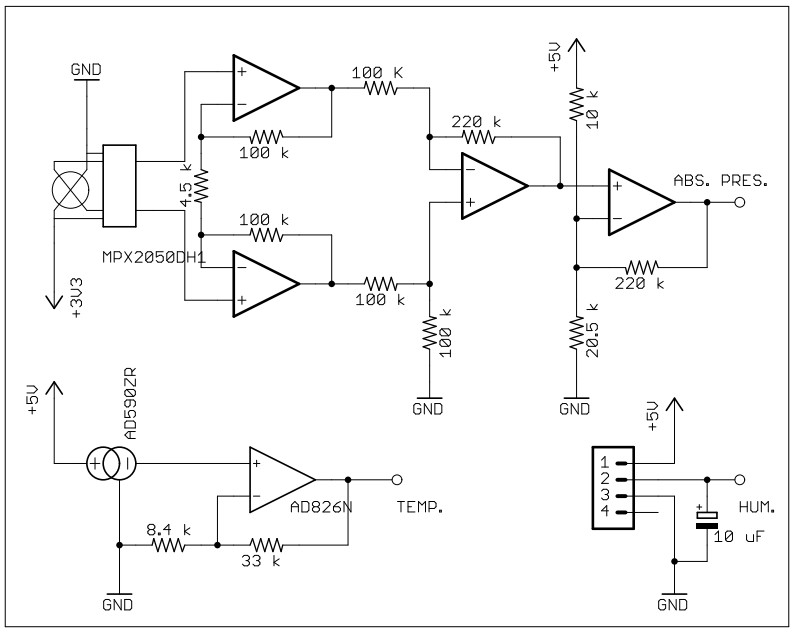

Figure 3.12: The Sensor Unit Circuitry

Nationals' LM35 temperature sensor was used for measuring the temperature. Due to small voltage span of LM35 (the sensitivity 10 mV/C°), an OP-AMP amplifier was used. For the measurement of the humidity a HSU-07C1-NMC3A analogue humidity sensor was used. This unit was calibrated with a CEM DT-172 commercial humidity and temperature logger. For the measurement of the absolute pressure,

MPX200A absolute pressure sensor from Motorola and a signal conditioning circuitry with LMC660 were used (Fig. 3.12). The outputs of all three sensor stages fed into analogue inputs of the datalogger. The schematics of the sensor unit is in the below.

3.1.6 The Logic Counter Circuit

The three atmospheric parameters (humidity, temperature and absolute pressure) should be measured for the correlation analysis in addition to the digital count rate. A datalogger with a Programmable Interface Controller (PIC) with 4 analogue inputs interfaced to an SD card was used for storing the data. For that reason, the digital count rate information was converted to an analogue value. A two 4 bit TTL counter (74LS393) was used for counting the pulses from alphas and 8 bit digital count information was converted to an analogue value between 0 and 5V using DAC0800, a digital analogue converter. Figure 6 shows the circuit diagram of the counter circuitry (Fig. 3.13).

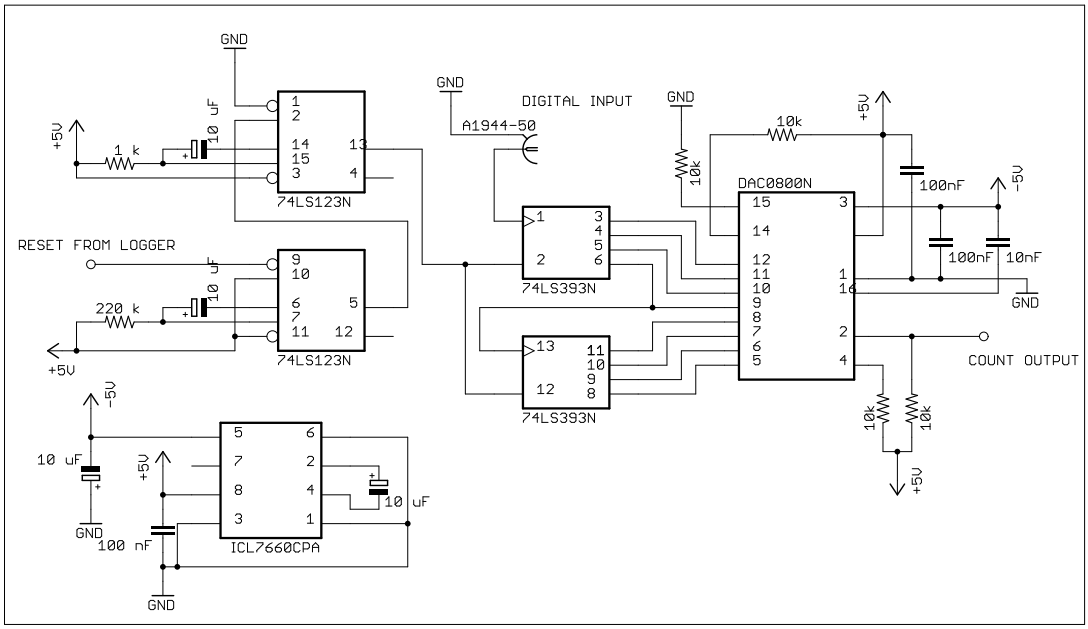

Figure 3.13: The Logic Counter Circuitry

3.1.7 Datalogger

The Radon field monitor has the ability of making four different measurements: alpha counts, temperature, relative humidity and absolute pressure. Because the device is portable and it is going to work in rural locations, the data has to be stored some way. A datalogger was constructed using a microcontroller unit (PIC18F452) and has four analogue input channels. Each channel can detect values between 0-5V and can save the data and time in text format. Measurements can be saved for certain time periods

and all the operations can be followed by an LCD screen. A reset signal for the counter is also obtained from the microchip.

3.1.8 Mains Filter

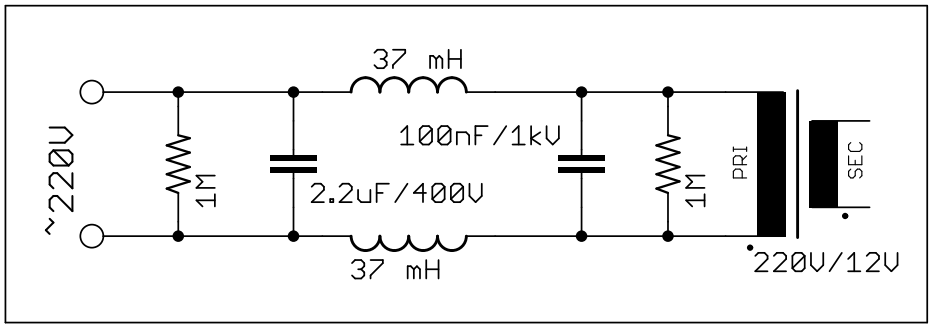

Figure 3.14: The mains medical filter circuitry

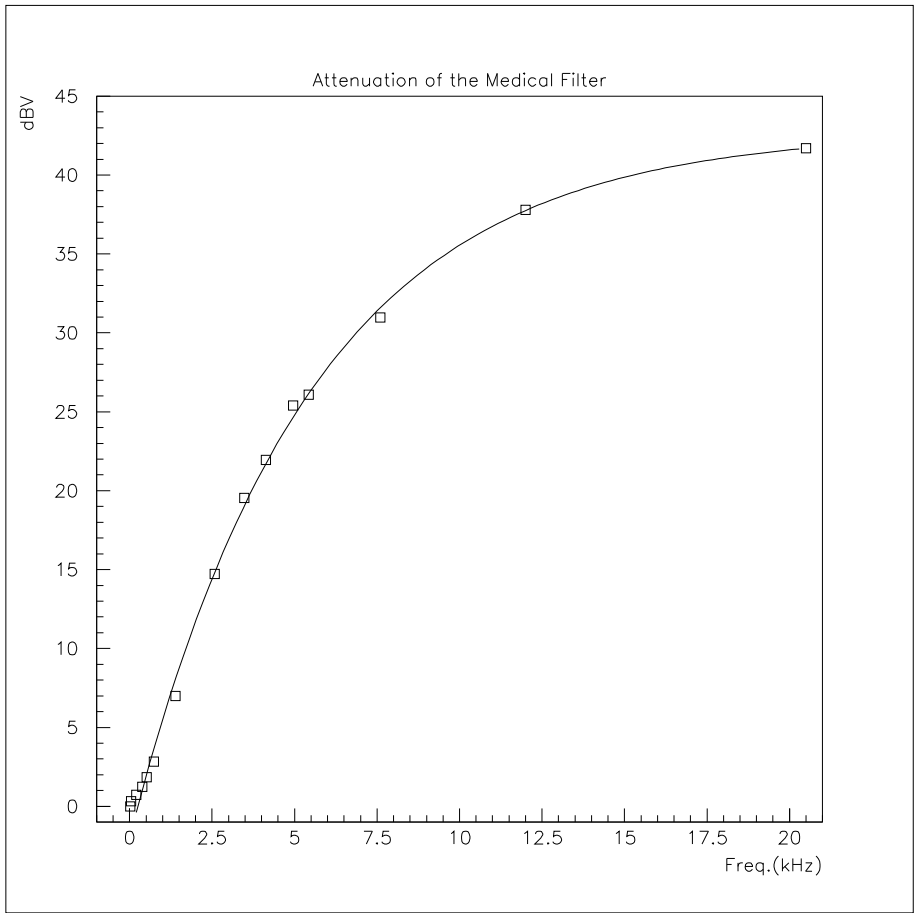

Figure 3.15: The Medical Filter Performance Test

The noise from the power line was eliminated using a simple medical mains filter (Fig. 3.14). Fast voltage spikes may occur with the sudden changes of the current in the power lines and these spikes may cause fake counts in the radon monitor. Since the amplitude of these spikes are large, they can not be eliminated completely by the step down transformer used for the power source from the mains. Figure 3.15 shows the performance of the filter.

3.2 Principle of Operation

Radon monitor operates with 12V DC power supply and there are two sources, mains power and a 12V/7A battery. A battery was integrated to the monitor against power cuts. But the device has the ability of doing measurement in rural areas in where it is difficult to find the mains power. For such conditions we also integrated a solar panel to the device. Thus, during the day battery supplies the module and is recharged by the solar panel at the same time. In the night battery goes on to supply the device without recharge.

The main operation principle of the device depends on the continuous sampling of the ambient air. An air pump takes in the air from the inlet and carry to the detection chamber with a speed of 1 l/min (Figure 3.16).

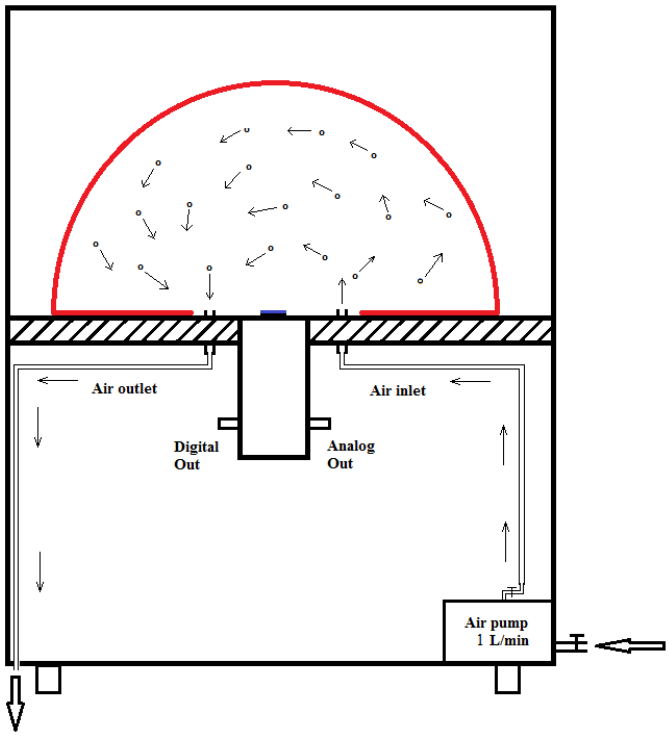

Figure 3.16: General view of Radon monitor internal structure.

Measurement chamber indicates a strong electric field generated by the application of +3500 V DC to the metal hemisphere and locating the detector to the middle of the wood shelf. Since the photodiode carry a much lower voltage, a strong electric field directed to the detector surface was constructed. Since the range of alpha particles in the air is very short, we aimed to collect electrostatically the positive ionized Polonium atoms close to the photodiode. In this way, alpha particles from their decay will be able to reach to the photodiode and create the corresponding signal.

We also measure the atmospheric parameters of the measurement location. This is achieved by the usage of a sensor card including a temperature sensor, a humidity sensor and an absolute pressure sensor. In the end we record all the measurements on an SD card by using the datalogger circuit card. Datalogger also record the time and date of the measurement and also let us to define the sampling period.

4. PERFORMANCE TESTS OF THE MONITOR

Tests of the circuits were performed individually. Since the detector circuitry was the heart of the radon monitor, the most crucial tests took place for this circuit. The noise, the effect of temperature, humidity and absolute pressure were the most important issues.

4.1 Detector Noise

Figure 4.1 shows the snapshot of the single detector noise taken for 1 ms.

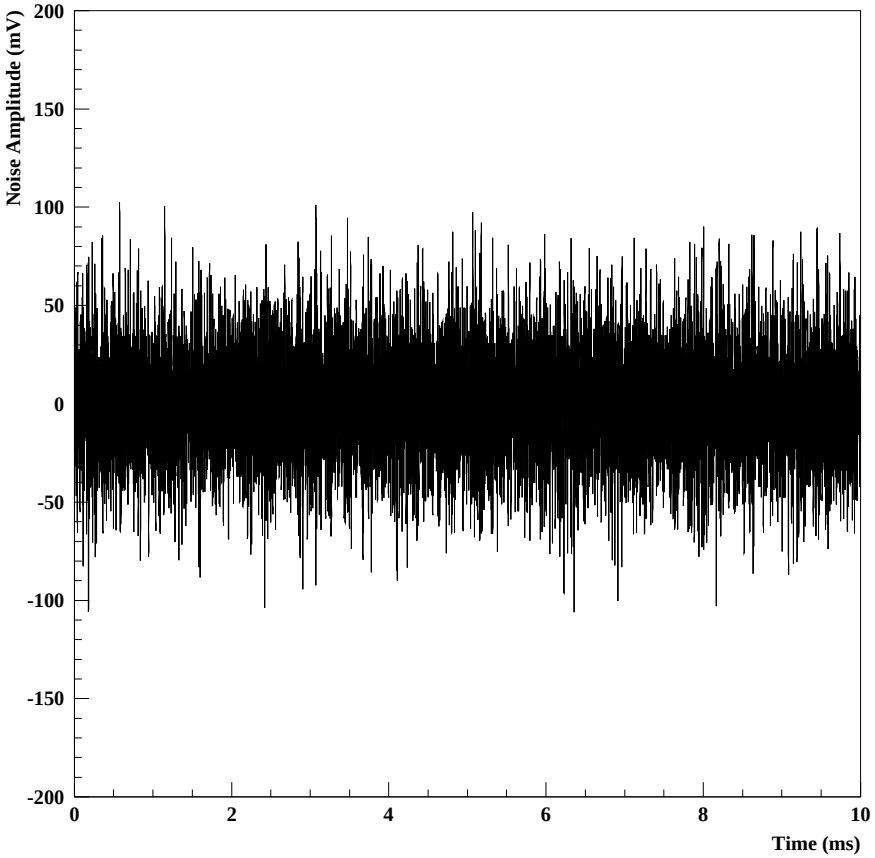

Figure 4.1: 1 ms detector noise fourier spectrum

Figure 4.2 was obtained from the average of the projections of the many noise spectra given. As it is expected, the distribution is a good Gaussian and the noise RMS is about 27 ± 1 mV. This measurement was performed at the output of the shaping amplifier. There wasn't much difference between the Fourier spectra with and without HV-on, except the 9 kHz component due to the clock signal of the high voltage power supply.

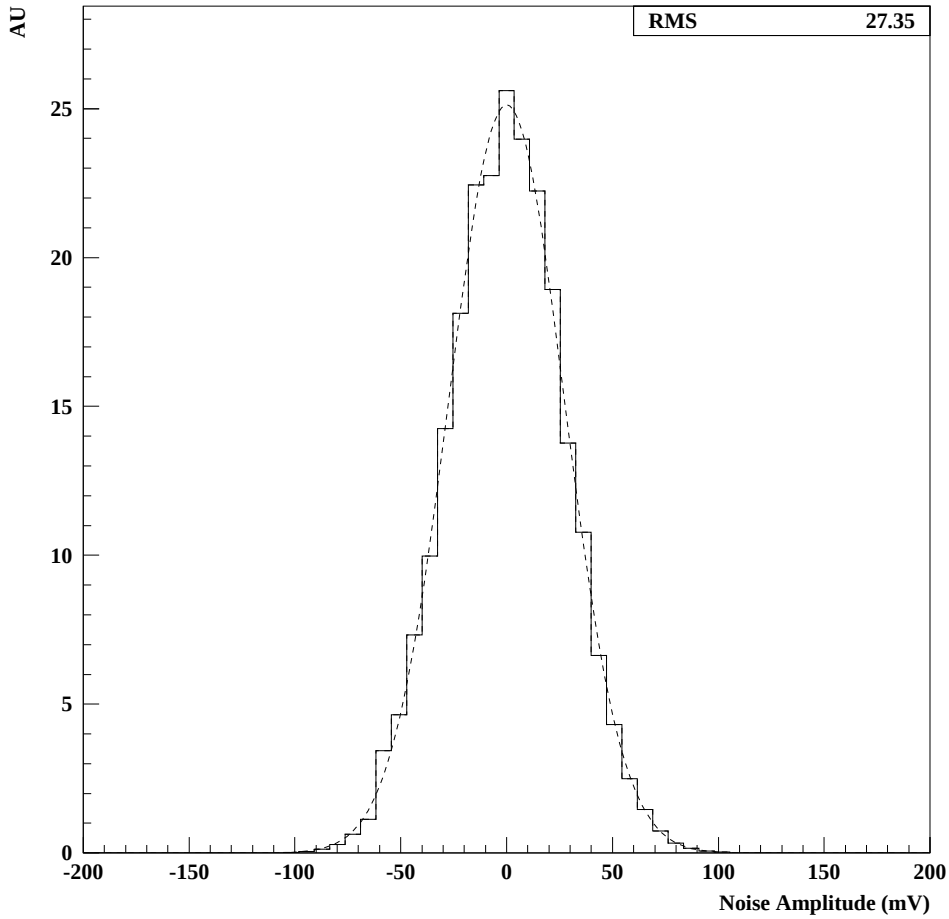

Figure 4.2: 1 ms detector noise projection

Amplitude of the HV clock signal in the Fourier Spectrum is smaller than the maximum detector noise which is around 120 kHz. It has to be pointed out that our detection threshold for alphas from radon daughters was set to 1V where the RMS level of the detector noise was only 30 mV.

There is a strong correlation between the temperature and the detector noise. Figure 4.3 shows the RMS value of the noise vs the temperature. As seen from the figure, there is a linear correlation between the RMS value of the noise and the temperature.

4.2 Measurements

The tests of the detector was performed with a 5 μCi ^{226}Ra source. The source is positioned next to the photodiode. Figure 4.4 shows the average signal induced from the 4.78 MeV alpha rays of ^{226}Ra source.

There is only one strong gamma line (411 keV) in the decay chain of the ^{226}Ra which belongs to the mother nucleus. Any spectra taken with radium source contains noise,

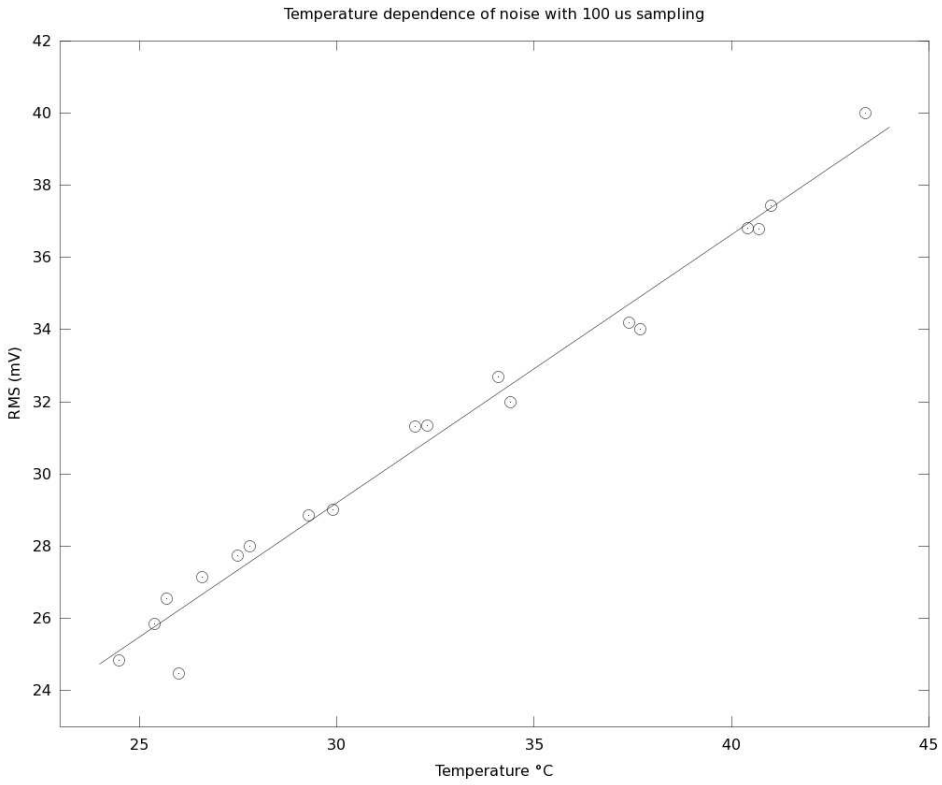

Figure 4.3: Dependence of RMS value to the temperature with 100us sampling rate.

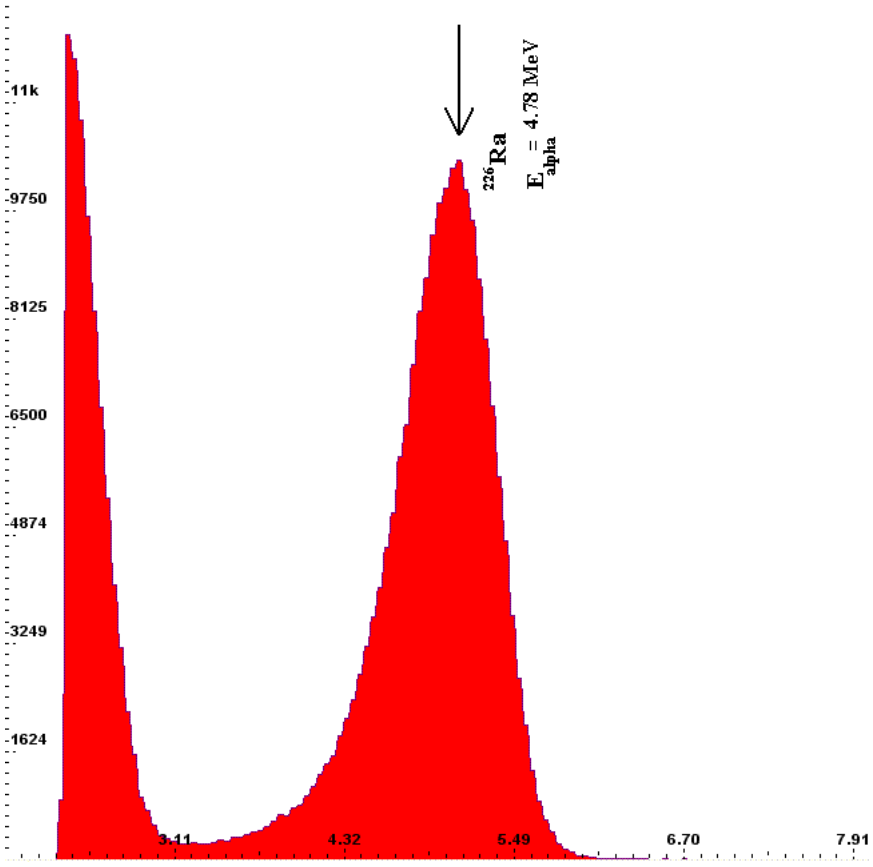

Figure 4.4: ^{226}Ra spectrum

411 keV gamma line and lines from the decay products of the daughter nuclei. Luckily, the efficiency of the detector for gamma rays is very small compared to the one for alphas. However, the following study was performed to determine the right threshold for the comparator to eliminate the noise and the possible gamma interference from the radon counts.

It is known that large fraction of the daughter nuclei ^{218}Po and ^{214}Po of ^{222}Rn become positively charged and a static electric field can be used to collect them near the photodiodes. This way, most of the decay products can be forced to move directly on towards the photodiode. The DC potential for this purpose can be couple of thousands of volts depending on the size and shape of the collection chamber. Application of the high voltage to provide electric field increases the sensitivity of the radon detection. Humidity and temperature play important role for the detection of the radon.

5. FIELD MEASUREMENTS

Finalizing the prototype device was followed by building ten more Radon Field Monitors. They were positioned at 10 different locations in the İstanbul Technical University Ayazağa Campus. The radon measurements have been performed for nearly two months in each station. We considered several issues for the determination of the locations where we located 10 RSM modules. Since higher concentration was expected in the locations with inadequate ventilation, we have chosen the basements of the buildings. The way these locations are not continuously used by the people let us made our measurements disturbance free.

5.1 Count vs Time

The following six figures show some of the measurements. Y-axis corresponds to the counts per hour and X-axis shows the elapsed time in the units of months.

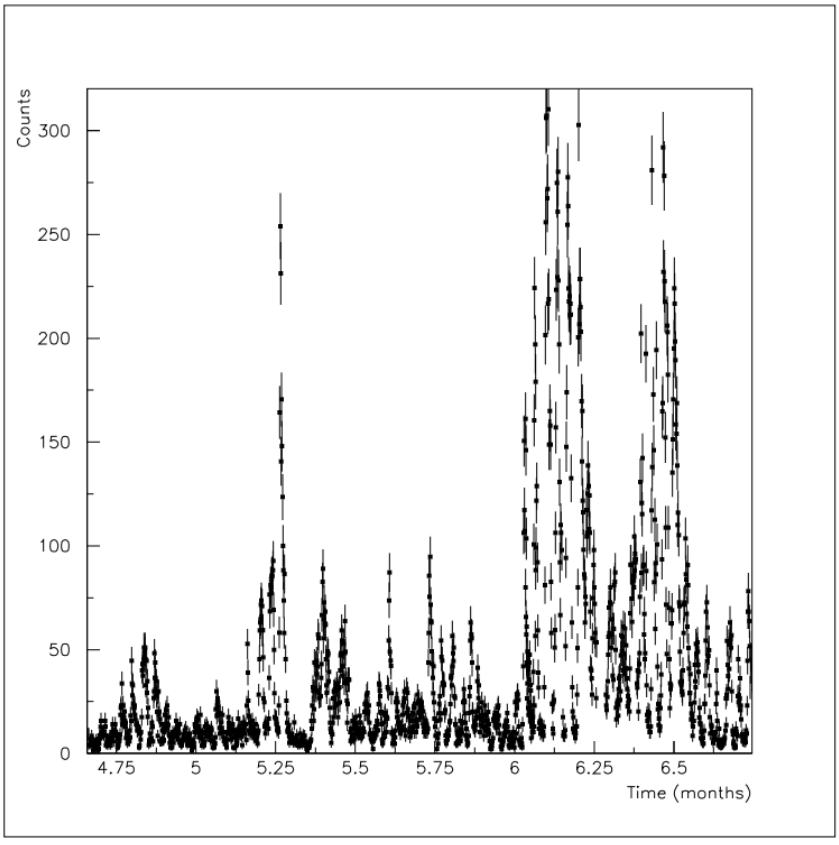

Figure 5.1: Radon measurements in the basement of Physics Seminar Room of the Faculty of Science and Letters.

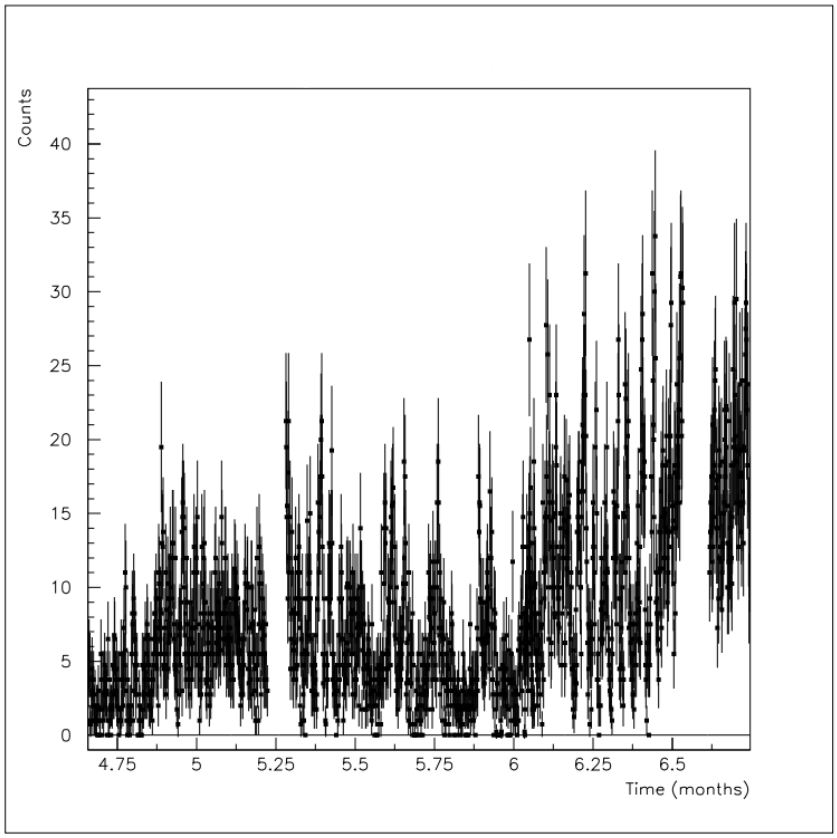

Figure 5.2: Radon measurements in the basement of the Molecular Biology and Genetics Department of the Faculty of Science and Letters.

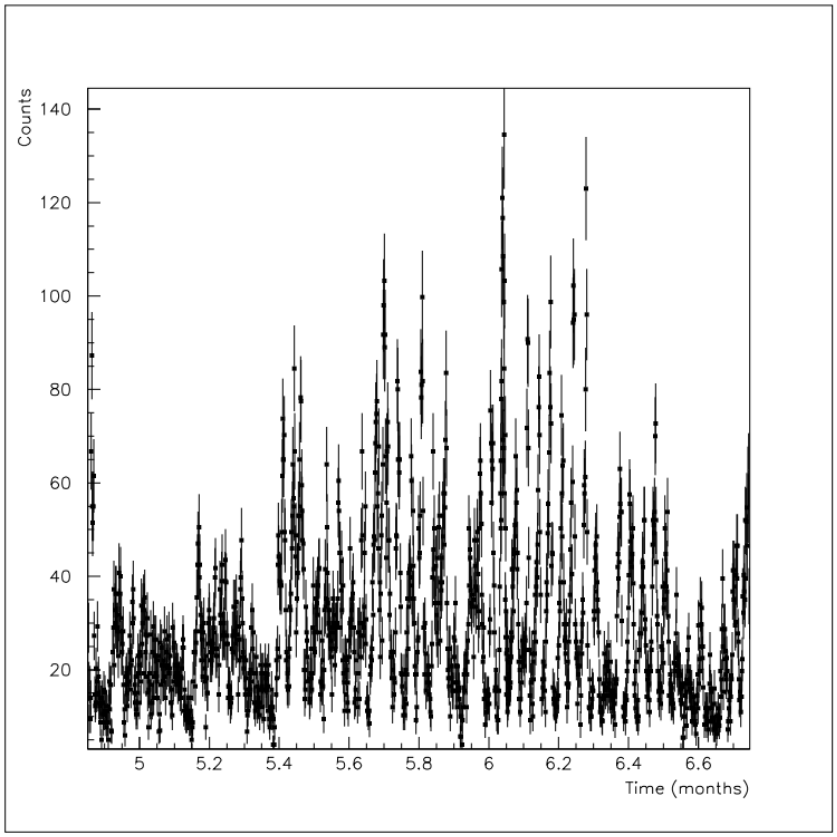

Figure 5.3: Radon measurements in the tunnel between the Faculty of Chemical and Metallurgical Eng. and the Faculty of Naval Architecture and Ocean Eng.

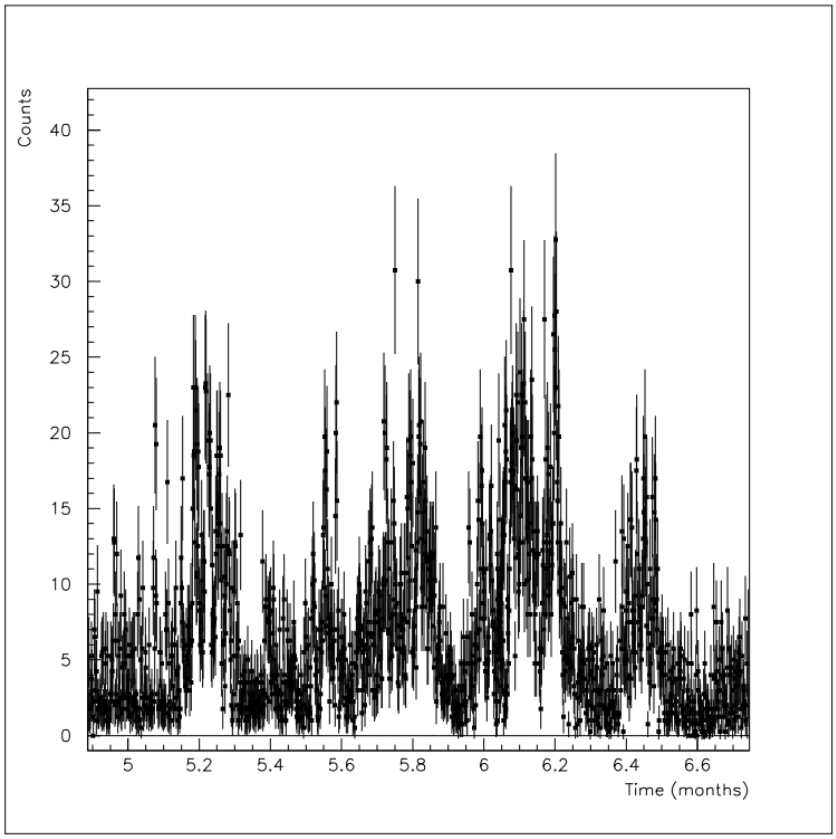

Figure 5.4: Radon measurements in the Seminar room of the Physics Department.

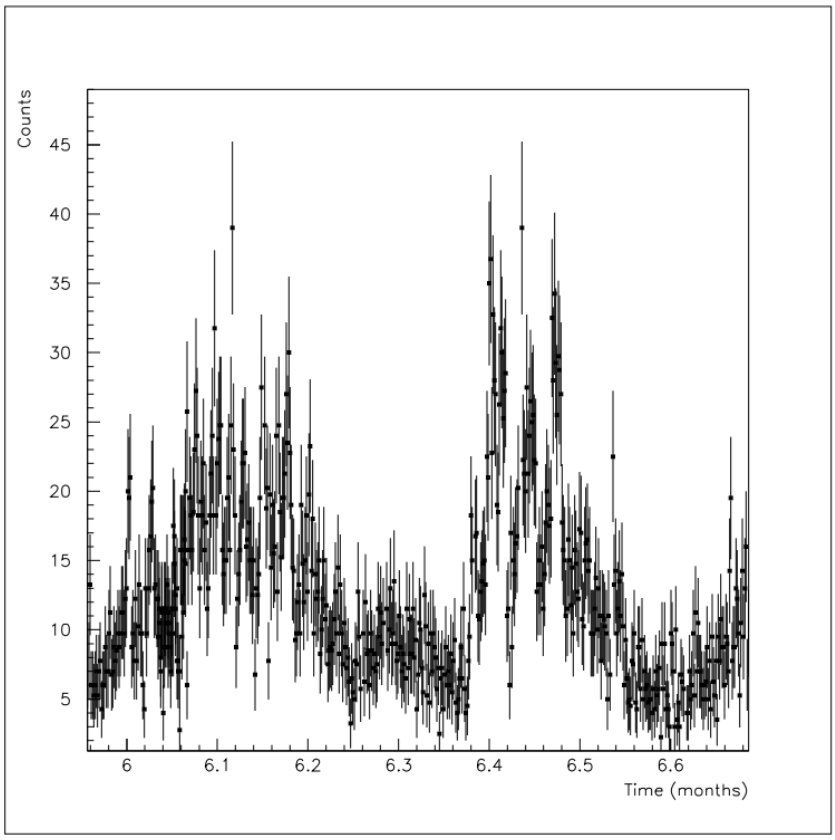

Figure 5.5: Radon measurements in the furnace room of the Faculty of Mine Engineering.

Figure 5.6 shows the atmospheric measurements together with counts. From upper left to the lower right figures are correspond to radon counts, temperature, humidity and pressure. Athmospheric parameters are uncalibrated relative measurements.

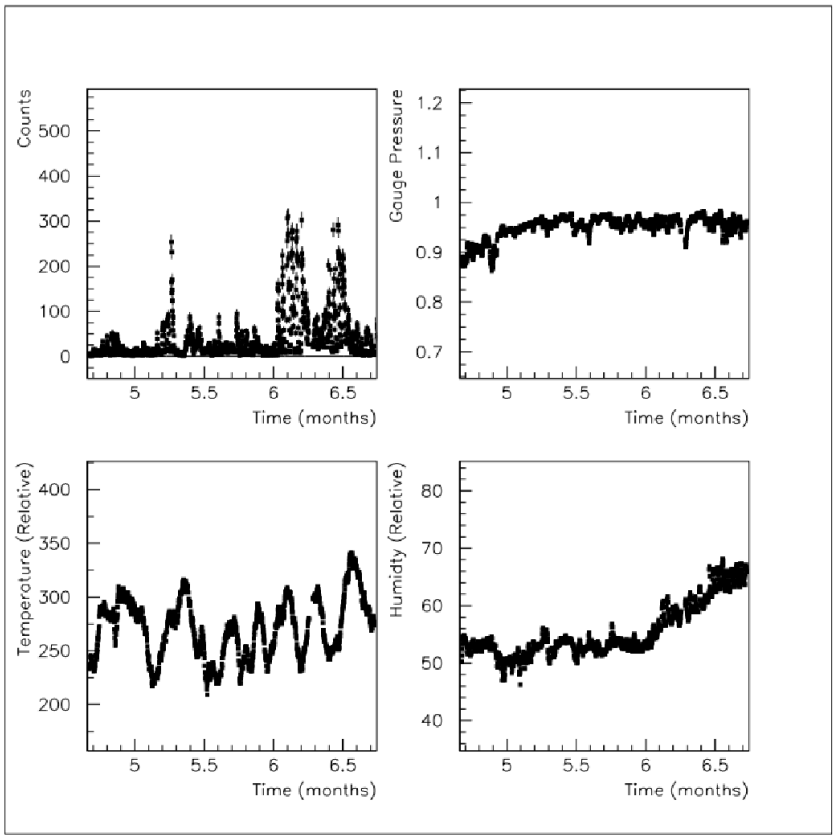

Figure 5.6: Recorded radon counts together with atmospheric measurements in the basement of Physics Seminar Room of the Faculty of Science and Letters.

6. CONCLUSION

The Radon Field Monitor Project after 2.5 years has come through the end of phase 1: materialization of prototype device and first field measurements.

We can divide this long period into two sections. In the first stage the individual tests of the circuits were performed and all the electronics were mounted into the case and tested as whole in the second stage.

6.1 Phase 1

We spent most of our time on the design and optimization of the alpha detector. We started from the result of a previous thesis work, entitled with *Gamma-ray Detector Array*, materialized in the same laboratory by ANGÜNER, E. O. under the advisory of Prof. Dr. OZBEN, C. Ş. [33]. Gamma-ray detector is also based on a silicon PIN photodiode and has similar amplification stages as transempedance and shaping amplifier with the alpha detector. However, since the interaction of charged particles with matter is much different than the gamma rays, we had to optimize it for alpha detection.

Our first task was to find the suitable photodiode and the op-amp. We used the same op-amp with a JFET input stage but decided to use another photodiode. Difficulty of finding the same photodiode was the reason of it. However, the new one with a larger active surface it became much more efficient with the detection of alphas.

The PCB design of the detector needed much more attention. The very small signal output of the photodiode was the reason for this extra care. The careful design of the detector PCB was crucial on our work. For this reason we tested various PCB design experimentally.

Stability problems were arising from the electronic noise and the interference with electromagnetic waves. At this point usage of a metal box, another word Faraday cage, solved most of the problems. Individual tests of the detector devices carried out in the dark.

As it was described in chapter 3, the alpha detector can provide two outputs, analog and digital. Then the digital output was obtained with a comparator IC. We adjusted all detectors individually by setting proper threshold to the comparator.

At the end of these works we moved to prepare an MCA output since the impedance mismatch results in the loss of detector signal. Thus we add an extra amplification stage to the both outputs, analog and digital signals. At the end we obtained good signal output on both the oscilloscope and the alpha spectrum of ^{226}Ra.

High voltage power supply was the second most challenging unit in the device which we spent much of our time. Since the high voltage unit generates +3500V DC supply, especially the cascade stage needed more care against discharges. Obtaining a stable output and conveying this high voltage in the monitor was other problems that we met.

We left some distance between the capacitors by taking into account the discharge between oppositely charged electrodes of the capacitors. Also we add a high value of resistor to the output stage for a better stability. Since an open end behaves like an antenna we observed that addition of such high value of resistor was really useful but didn't solved the whole problem. Although we got a smaller ripple voltage it was still affecting the detector as fake counts. As a last step we connected an RC filter circuit to the output. The filter circuit gave the best result. At the end we observed several volts of oscillation. After completing these two important steps we started to develop other supporting circuits.

6.2 Phase 2

The individual test of each unit in the monitor resulted really well. Then we combined them all in a plastic box covered with opaque photography papers. The first problem we met was the interference due to other devices working on the same power line. We tested this in detail by connecting and removing each device on the same line. When some of them were working we observed so many counts even. We also test the condition when we operate the device from a battery. There were no problems in this condition.

We found out the problem with the help of Fourier transform of the detector noise spectrum. We observed that the problem arise from the high frequency components in the power line. This initial problem was solved by using a so called medical filter

at the power line input stage. We had some problems also on the light leakage. Thus during the early days of the monitor we used a thick coat to keep the detector from light leakages.

We observed some other problems internally in the device. One of them was originated from the high voltage power supply which process a 9 kHz signal. In the detector noise spectrum we also observed this signal. A similar problem also appeared at the counter circuit since it has a pulse source inside. We solved these problems by changing the power supply paths and including some passive circuit components which provide filtering for high frequencies.

We investigate the position of the detector to improve the detection efficiency. First condition was placing the active surface of the detector, the photodiode surface, at the same level with the shelf upper surface. This became also our final choice. We compared the other conditions with this one.

We also tested the case that a negative high voltage applied to the grid and the dome (upper spherical shell) was grounded. Unfortunately this case did not provide any better result.

6.3 Future Plans

We can express our future plans under two titles: Developing the Radon Field Monitor further more and Field Measurement projects.

Now the Radon Field Monitor works very well in the field, however; there are some points that we want to improve. The first one of them is increasing the detection/collection efficiency. Because of the large surface of the ground plate near the detector, the field is not focused on the detector active surface perfectly. By confining the ground plate to the active surface would increase the collection efficiency significantly.

Most of the works in the literature use negative high voltage for the collection vessel which presumably increases the detection efficiency for the reason explained above. This requires very smooth power supply (expensive) for feeding the leads of photodiode.

Optimization of the detector signal is another point we want work on. Especially for the spectroscopic applications we want to get a better output.

As a third one we consider to develop a better data management process possibly with a communication unit. This unit will not only record the data but also send it to a remote center. This will let us to locate the monitors remote locations. It can be also possible to control and direct the device from the remote center. A better physical appearance with an easy to use interface is in our long term plan, too.

Field measurement projects were our basic motivation in the beginning. A Radon measurement network along with active fault zones in Turkey, especially on the North Anatolian Fault Zone, is our initial aim. In this network we plan to establish thousands of Radon Field Monitors from one end to the other of the Fault zone and real track follow the Radon level. We have a similar plan also for Marmara Region since Istanbul is under the risk of a strong earthquake. On the other hand, we would like to widen this network because of two reasons. One of them is that as known Turkey is located on several earthquake zones. Thus it is better to widen the network and to establish as many as possible monitors all over Turkey. The second one is when we widen this network it will be also possible to prepare Radon maps of some locations of Turkey.

REFERENCES

[1] **Meyerhof, W.E.**,(1989). *Elements of Nuclear Physics*, McGraw-Hill, New York.

[2] **Krane, K.S.** (1988). *Introductory Nuclear Physics (3rd Ed.)*. Wiley, New York.

[3] **Blin-Stoyle, R.J.** (1991). *Nuclear and Particle Physics*. Chapman & Hall, London.

[4] **Bertulani, C.A.** (2007). *Nuclear Physics in a Nutshell*. Princeton Uni. Pr., New Jersey.

[5] **URL-1**, <*http://www.epa.gov/safewater/radionuclides/training/module4/index.html*>, date retrieved 15.04.2012.

[6] **Knoll, G.F.** (2000). *Radiation Detection and Measurement (3rd. Ed.)*. Wiley, London.

[7] **URL-2**, <*http://www.globalspec.com/reference/13668/160210/chapter-9-2-semiconductor-basics*>, date retrieved 15.04.2012.

[8] **Jevremovic,T.** (2005). *Nuclear Principles in Engineering (2nd. Ed.)*. Springer, USA.

[9] **Aldenkamp, F.J.and Stoop, P.** (1989). *Sources and Transport of Indoor Radon: Measurements and Mechanisms*. Springer, Kröningen.

[10] **Leo, W.R.** (1994). *Techniques for Nuclear and Particle Physics - A How-To Approach (2nd Ed.)*. Springer, Germany.

[11] **Bacon, M.E.**, 2004. A comparison of electrostatic and filtered air collection of Radon progeny, *Eur. J. Phys.*, **25**, 239-248.

[12] **URL-3**, <*http://enhs.umn.edu/hazards/hazardssite/radon/radonmeasuremethods.html*>, date retrieved 22.04.2012.

[13] **Sanchez,A. M., Poncela L. S. Q.** , 2011. Radon: Risks and Applications, *Nuclear Physics News Magazine*, **21**, (3), 17-22

[14] **URL-4**, <*http://www.doh.wa.gov/ehp/rp/factsheets/factsheets-htm/fs10bkvsman.htm*>, date retrieved 20.04.2012.

[15] **URL-5**, <*http://www.tennesseeradontesting.com/radon-enters.jpeg*>, date retrieved 20.04.2012.

[16] **WHO: World Health Organisation** (2009). *Handbook on indoor Radon: A public health perspective*. WHO Press, France.

[17] **Ghosh, D., Deb, A., Sengupta R.**, 2009. Anomalous radon emission as precursor of earthquake, *Journal of Applied Geophysics*, **69**, 67-81

[18] **Shiratoi, K.**, 1927. The variation of radon activity of hot spring, *Science Reports of the Tohoku Imperial University*, Series 3 **16**, 614-621

[19] **Hatuda, Z.**, 1953. Radon content and its change in soil air near the ground surface., *Memoirs of the College of Science, University of Kyoto*, Series B **20**, 285-306

[20] **Ulomov, V I. and Mavashev, B. Z**, 1967. Precursor of a strong tectonic earthquake., *Acad. Sci. USSR, Doklady, Earth Sci. Sec*, **176**, 9-11.

[21] **Asimov, M.S., Yerzhanov, Zh.S., Kalmurzaev, K.Ye., Kurbanov, M.K., Mavlyanov, G.A., Negmatullaev, S.Kh., Nersesov, I.L., Ulomov, V.I.**, 1979. The state of earthquake prediction research in the Soviet Republics of Central Asia, *Int. Symposium on Earthquake Prediction, Rep. III-12. UNESCO, Paris*, 20.

[22] **Wakita, H., Nakamura, Y., Notsu, K., Noguchi, M., Asada, T.**, 1980. Radon anomaly: a possible precursor of the 1978 Izu-Oshima-kinkai earthquake, *Science*, **207**, 882-883.

[23] **Fleischer, R.L., Mogro-Campero, A.**, 1985. Association of subsurface radon changes in Alaska and the north-eastern United States with earthquakes, *Geochimica et Cosmochimica Acta*, **49**, 1061-1071.

[24] **Friedmann, H., Aric, K., Gutdeutsch, R., King, C.Y., Altay, C., Sav, H.**, 1988. Radon measurements for earthquake prediction along the North Anatolian Fault Zone: a progress report, *Tectonophysics*, **152**, (3-4), 67-81.

[25] **Hirotaka, Ui., Moriuchi, H., Takemura, Y., Tsuchida, H., Fujii, I., Nakamura, M.**, 1988. Anomalously high radon discharge from the Atotsugawa fault prior to the western Nagano Prefecture earthquake (M=6.8) of September 14, 1984., *Tectonophysics*, **152**, (1-2), 147-152.

[26] **Igarashi, G., Saeki, S., Takahata, N., Sumikawa, K., Tasaka, S., Sasaki, Y., Takahashi, M., Sano,Y.**, 1995. Groundwater radon anomaly before the Kobe earthquake in Japan, *Science*, **152**, (269), 60-61.

[27] **Virk, H.S., Walia, V.**, 2001. Helium/radon precursory signals of Chamoli earthquake, India, *Radiation Measurements*, **34**, 307-384

[28] **Agrawal, G.P.** (2002). *Fiber-Optic Communication Systems (3rd. Ed.)*. Wiley, London.

[29] **Martin-Martin, A., Gutierrez-Villanueva, J.L., Munoz, J.M., Garcia-Talavera, M., Ademiec, G., Iniguez, M.P.**, 2006. Radon measurements with a PIN photodiode, *App. Rad. & Isotopes*, **64**, 1287-1290.

[30] **Takeuchi, Y., Okumura, K., Kajita, T., Tasaka, S., Hori, H., Nemoto, M., Okazawa, H.**, 1999. Development of high sensitivity radon detectors,

Nuc. Ins. & Meth. in Phys., A **421**, 334-341.

[31] **Mitsudad C., Kajitab T., Miyanod K., Moriyamaa S., Nakahataa M., Takeuchia Y., Tasakac S.**, 2003. Development of super-high sensitivity radon detector for the Super-Kamiokande detector, *Nuc. Ins. & Meth. in Phys.*, A **497**, 414-428.

[32] **Takeuchi, Y.** (2004) **Okumura, K.**, **Kajita, T.**, **Tasaka,S.**, **Hori, H.**, **Nemoto, M. and Okazawa, H.**. A comparison of electrostatic and filtered air collection of Radon progeny, *Nuc. Ins. & Meth. in Phy. Res. Sec. A* , **421**, 334-341.

[33] **Angüner, E.O.**, 2008. Gamma-ray dedector array, Master's thesis, İTÜ, İstanbul, Turkey

CURRICULUM VITAE

Name Surname: Ahmet BAYRAK

Place and Date of Birth: Sinop / 23.01.1985

Adress: İstanbul Technical University, Science and Letters Faculty,
Physics Engineering Department, B4-101, İstanbul/TURKEY

E-Mail: bayrakah@itu.edu.tr

B.Sc.: ITU Physics Engineering Department, 2009

List of Publications and Patents: Radon Saha Monitörü (Applied).

PUBLICATIONS/PRESENTATIONS ON THE THESIS

- İzmir Yüksek Enerji Fiziği ve Uygulamalari Çalıştayı, (İZYEF - 2012), 19-23 June 2012